Synthesis, Characterization, Critical Micelle Concentration and Biological Activity of two-Headed Amphiphiles

Marcelo Luis Actis

Thesis submitted to the Faculty of the Virginia Polytechnic Institute and State University
in partial fulfillment of the requirements for the degree of

Master of Science

in

Chemistry

Richard D. Gandour, Chairman
Paul R. Carlier, Member
Felicia Etzkorn, Member

November 6, 2008
Blacksburg, VA 24061

Keyword: two-headed, di-carboxylato, amphiphile, critical micelle concentration, antimicrobial activity, *S. aureus*, MRSA

Copyright 2008, Marcelo L. Actis

Synthesis, Characterization, Critical Micelle Concentration and Biological Activity of two-headed Amphiphiles

Marcelo Luis Actis

ABSTRACT

In this project, we synthesized a new homologous series of five long-chain, two-headed amphiphiles [**2CAm13**, **2CAm15**, **2CAm17**, **2CAm19**, **2CAm21**; $CH_3(CH_2)_{\mathbf{n}\text{-}1}CONHC(CH_3)(CH_2CH_2COOH)_2$, **n** = 13, 15, 17, 19, 21]. The synthesis of the **2CAmn** series was accomplished in four steps. The first step involves a reaction of nitroethane and two equivalents of *tert*-butyl acrylate to create the nitrodiester synthon [$O_2NC(CH_3)(CH_2CH_2COO^tBu)_2$] by successive Michael additions. The second step in the synthesis consists of a reduction of nitrodiester with H_2 and Raney nickel to give the diesteramine [$H_2NC(CH_3)(CH_2CH_2COO^tBu)_2$]. The third step is the condensation of an acid chloride with diesteramine to give an alkanamido diester [**2EAmn**; $CH_3(CH_2)_{\mathbf{n}\text{-}1}CONHC(CH_3)(CH_2CH_2COO^tBu)_2$, **n** = 13, 15, 17, 19, 21]. The final step is the removal of the *tert*-butyl protecting groups to give **2CAmn**.

Critical micelle concentration measurements were collected by the pendant drop method for measuring surface tension for a series of triethanolamine/**2CAmn** solutions to establish the concentration required for detergency. The CMCs for the **2CAmn** series were found to decrease in value from 3.0×10^{-2} M (**2CAm13**) to 1.7×10^{-4} M (**2CAm21**) in a linear fashion [log CMC = $(-0.28 \pm 0.01)\mathbf{n} + (2.2 \pm 0.1)$]. The CMCs for the **2CAmn** series falls in between the CMCs for three series of homologues three-

headed amphiphiles (**3CAmn**, **3CCbn**, **3CUrn**) and the CMCs for fatty acids, with fatty acids having the lowest CMCs.

Antibacterial activity (minimal inhibitory concentrations, MICs) for a series of homologous dendritic two-headed amphiphiles and three series of homologous, three-headed amphiphiles against *Staphylococcus aureus* and methicillin-resistent *S. aureus* (MRSA) were measured by broth microdilution to compare the effect of chain length and, hence, hydrophobicity. Inoculum density affected antibacterial activity of the **2CAmn** series against both *S. aureus* and MRSA. MIC measurements at different cell densities showed that activity decreased with higher cell densities. For all four series, the MICs were relatively flat at low inoculum densities. This flat region defines the intrinsic activity, MIC_0. The MIC_0 results revealed that inoculum density, chain-length, and hydrophobicity all influenced antibacterial activity and that activity correlates strongly with clogp, an established measure of hydrophobicity. The most hydrophobic members from each homologous series exhibited antibacterial activity. The most active homologue of the **2CAmn** series was **2CAm21** with MIC_0 of 2.0 ± 1.0 and 3.2 ± 1.0 μM against *S. aureus* and MRSA, respectively.

The CMCs and MIC_0s of the two- and three-headed amphiphiles were compared for both *S. aureus* and MRSA to gauge the effect that micelles may have on activity. Amphiphile **2CAm19** has the largest ratio between CMC and MIC_0 ($CMC/MIC_0 = 205$) against *S. aureus* and **3CUr20** has the largest ratio ($CMC/MIC_0 = 339$) against MRSA. These ratios suggest that micelle formation is not a mechanism of action for anti-*Staphylococcal* activity.

Acknowledgements

I would like to thank my wife, Krystal Actis, for her support and encouragement during my time at Virginia Tech. As a nurse, Krystal helped me get a new perspective on the importance of the work done by the Gandour group. I would like to thank my parents, Luis and Gloria Actis, for their support of my goals. I would also like to thank them for inspiring me to choose a career path in which I can make a positive contribution to society. I would also like to thank my brother, Gustavo Actis, for his support.

I would like to thank my advisor, Dr. Richard D. Gandour, who has been a great source of knowledge. I have learned so much during my time with the group and I have enjoyed passing on that knowledge to other undergraduate and graduate students. I would especially like to thank Dr. Gandour for always being available for advise and support.

I would like to thank my lab partners who have helped me throughout my project. Dr. André Williams, Richard Macri, and Shauntrece Hardrict have all been great sources of information and advise. I would also like to thank, Brad Maisuria, Aaron Commons, and William Cang.

Additionally, I would like to thank Dr. Joseph Falkinham III for allowing the Gandour group the use of his lab for microbial assays. I would like to thank Myra Williams for her work in collecting data and results.

Finally, I would like to thank my masters committee, Dr. Paul Carlier and Dr. Felicia Etzkorn, for their guidance.

Dedication

I would like to dedicate this document to my wife, Krystal Actis, my grandparents, Mario Bohne, Gloria Bohne, and Angela “Lita” Actis, and my parents, Luis and Gloria Actis.

Table of Contents

List of Figures viii
List of Tables ix
List of Schemes x

Chapter 1: Background, Critical Micelle Concentration, and Antimicrobial Activity of Amphiphiles 1
1.1 Goals and Introduction 1
1.2 Introduction to Amphiphiles 4
1.3 Aqueous Solubility 6
1.4 CMCs of Multi-headed, Anionic Amphiphiles 7
1.5 Introduction to *Staphylococcus aureus* and Methicillin-Resistant *Staphylococcus aureus* 10
1.6 Antimicrobial Activity of Fatty Acids against *S. aureus* 12
1.7 Antimicrobial Activity of Fatty Acids against MRSA 13
1.8 Antimicrobial Activity of Dendritic Amphiphiles Against *S. aureus* 13
1.9 Antimicrobial Activity of Dendritic Amphiphiles Against MRSA 14
1.10 Conclusion 15
1.11 References for Chapter 1 15
Chapter 2: Synthesis of the 2CAmn Series 19
2.1 Introduction 19
2.2 Formation of Nitrodiester 20
2.3 Formation of Diesteramine 21
2.4 Synthesis of Long-Chain Acid Chlorides 23
2.5 Formation of an Amide Bond Utilizing Diesteramine 23
2.6 Removal of the *tert*-Butyl Groups via two Methods 24
2.7 Overall Synthesis of the **2CAmn** Series 25
2.8 Comment on NMR Characterization: Diastereotopic Protons 26
2.9 General Comments for Synthetic Work 28
2.10 Experimental Procedure for the Formation of Di-*tert*-butyl 4-Methyl-4-nitroheptanedioate, Nitrodiester. Triton-B Procedure. 29
2.11 Experimental Procedure for the Formation of Di-*tert*-butyl 4-Methyl-4-nitroheptanedioate, Nitrodiester. DBU Procedure 30
2.12 Experimental Procedure for the Formation of Di-*tert*-butyl 4-Amino-4-methylheptanedioate, Diesteramine 31
2.13 Experimental Procedure for the Formation of Tetradecanoyl Chloride 31
2.14 General Procedure for the Formation of C_{16}–C_{22} Acid Chlorides 32
2.15 Experimental Procedure for the Formation of C_{16}–C_{22} Acid Chlorides 32
2.16 Experimental Procedure for the Formation of Di-*tert*-butyl 4-Methyl-4-(1-oxooctadecylamino)heptanedioate, **2EAm17** 33
2.17 General Procedure for the Formation of **2EAm13, 15, 19, 21** 34
2.18 Experimental Procedure for the Formation of **2EAm13, 15, 19, 21** 35
2.19 Experimental Procedure for the Formation of 4-Methyl-4-(1-oxooctadecylamino)heptanedioic Acid, **2CAm17** 37
2.20 General Procedure for the Formation of **2CAm13, 15, 19, 21** 38

2.21 Experimental Procedure for the Formation of **2CAm13, 15, 19, 21** 38
2.22 References for Chapter 2 40
Chapter 3: Critical Micelle Concentrations for the 2CAmn Series 42
3.1 Introduction to CMC 42
3.2 CMC Results 42
3.3 Impurities in CMC Measurements 46
3.4 Discussion of CMC Results 48
3.5 CMC General Methods 51
3.5.1 CMC Determination **2CAm21** 51
3.5.2 CMC Determination **2CAm19** 54
3.5.3 CMC Determination **2CAm17** 56
3.5.4 CMC Determination **2CAm15** 58
3.5.5 CMC Determination **2CAm13** 60
3.6 References for Chapter 3 62
Chapter 4: Minimal Inhibitory Concentrations (MIC) for the 2CAmn Series 64
4.1 Introduction to MIC 64
4.2 Results of MIC Measurements 64
4.3 Discussion 68
4.4 Conclusion 75
4.5 References for Chapter 4 76
Chapter 5: Summary and Conclusion 77
5.1 Summary 77
5.2 Conclusion 78
5.3 References for Chapter 5 79

List of Figures

Figure 1.1 Structure of the **2CAmn** series 1
Figure 1.2 A generic example of the cutoff effect 3
Figure 1.3 Structure of three-headed amphiphiles 3
Figure 1.4 General structure of an amphiphile 4
Figure 1.5 Amphiphile Aggregates 5
Figure 1.6 Structures of multi-headed amphiphiles studied by Shinoda 7
Figure 1.7 The effect of the number of headgroups on CMC 8
Figure 1.8 Structure of iminodiacetic acid derivatives 8
Figure 1.9 The effect of two headgroups on CMC 9
Figure 1.10 Examples of drugs used to treat MRSA 11
Figure 1.11 *S. aureus* MICs for three-headed amphiphiles at high inoculum density 14
Figure 1.12 MRSA MICs for three-headed amphiphiles at high inoculum density 15
Figure 2.1 ^{1}H NMR spectra for nitrodiester and nitrotriester 27
Figure 2.2 Three-dimensional representation of nitrodiester and nitrotriester 27
Figure 2.3 ^{1}H NMR spectra for diesteramine and triesteramine 28
Figure 2.4 ^{1}H NMR spectra of **2EAm17** and **2CAm17** 28
Figure 3.1 Drop shape at high and low surface tension. 43
Figure 3.2 IFT vs. log of amphiphile concentration for **2CAm21** 44
Figure 3.3 IFT vs. log of amphiphile concentration for **2CAm19** 44
Figure 3.4 IFT vs. log of amphiphile concentration for **2CAm17** 45
Figure 3.5 IFT vs. log of amphiphile concentration for **2CAm15** 45
Figure 3.6 IFT vs. log of amphiphile concentration for **2CAm13** 46
Figure 3.7 Possible effect of excess TEA on micelle structure. 48
Figure 3.8 CMC Comparison 49
Figure 3.9 Amphiphiles compared in Figure 3.10 50
Figure 3.10 CMC Comparison for the **2CAmn** series, amphiphiles reported by Shinoda, and Paleos. 50
Figure 4.1 Effect of initial *S. aureus* cell density for **2CAm21**. 66
Figure 4.2 Effect of initial MRSA cell density for **2CAm21** 66
Figure 4.3 MIC_0 comparison for *S. aureus*. 67
Figure 4.4 MIC_0 comparison for MRSA 68
Figure 4.5 Ionization equilibrium for **3CAm21** and **2CAm21** 70
Figure 4.6 MIC_0 against *S. aureus* versus clogp for monoanions of the various amphiphiles 71
Figure 4.7 MIC_0 against MRSA versus clogp for monoanions of the various amphiphiles 71
Figure 4.8 MIC_0 versus logD at pH 7.4 for two- and three-headed amphiphiles against *S. aureus* 73
Figure 4.9 CMC and MIC_0 comparison for **2CAmn** and **3CAmn**. 74

List of Tables

Table 1.1 Examples of anionic, cationic, nonionic, and zwitterionic amphiphiles.....4
Table 1.2 pH Solubility of amphiphiles.....6
Table 1.3 Summary of FA studies on *S. aureus*.....12
Table 2.1 Removal of *tert*-butyl groups via two methods.....24
Table 3.1 **2CAm21** Dilutions used for measurement of IFT.....53
Table 3.2 CMC Data for **2CAm21**.....54
Table 3.3 **2CAm19** Dilutions used for measurement of IFT.....55
Table 3.4 CMC Data for **2CAm19**.....56
Table 3.5 **2CAm17** Dilutions used for measurement of IFT.....57
Table 3.6 CMC Data for **2CAm17**.....58
Table 3.7 **2CAm15** Dilutions used for measurement of IFT.....59
Table 3.8 CMC Data for **2CAm15**.....60
Table 3.9 **2CAm13** Dilutions used for measurement of IFT.....61
Table 3.10 CMC Data for **2CAm13**.....62
Table 4.1 Concentration ratio (CMC/MIC_0) between CMC and MIC_0.....74

List of Schemes

Scheme 2.1 Retrosynthesis of the **2CAmn** series..... 19
Scheme 2.2 Published methods for preparing di-*tert*-butyl ester synthons..... 20
Scheme 2.3 Formation of nitrodiester using triton-B 21
Scheme 2.4 Michael additions using DBU 21
Scheme 2.5 Method for the formation of diesteramine used by Newkome..... 22
Scheme 2.6 The use of *tert*-butyl groups to prevent lactam formation..... 22
Scheme 2.7 Method used to prepare diesteramine 22
Scheme 2.8 Reduction procedure using heptane..... 22
Scheme 2.9 Preparation of long-chain acid chlorides..... 23
Scheme 2.10 Synthetic route for the preparation of **2EAmn**..... 24
Scheme 2.11 Removal of the *tert*-butyl group 25
Scheme 2.12 Synthesis scheme for the **2CAmn** series..... 26

Chapter 1: Background, Critical Micelle Concentration, and Antimicrobial Activity of Amphiphiles

1.1 Goals and Introduction

The purpose of this research project is to synthesize a new homologous series of two-headed, long-chain amphiphiles. In this project, we desire to synthesize five new amphiphiles (Figure 1.1). Critical micelle concentration (CMC) measurements will be performed on the **2CAmn** series (Figure 1.1) to determine if detergency is a factor in the biological activity of the series. Finally, biological activity against *Staphylococcus aureus* and methicillin-resistant *S. aureus* (MRSA) will be measured for the potential use of these amphiphiles as topical microbicides.

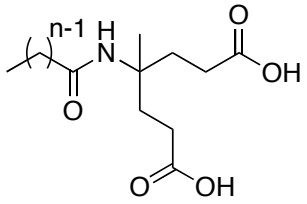

n = 13, 15, 17, 19, 21

Figure 1.1 Structure of the **2CAmn** series. Where **2C** = two carboxyl groups, **Am** = amido linker, and **n** = number of carbons in the alkyl chain

Amphiphiles are commonly referred to as surfactants. Ionic and nonionic surfactants find uses in a variety of applications[1]—detergents, shampoos, crude oil recovery enhancers, cosmetics, chelating agents[2], and antimicrobial agents[1, 3, 4]. In our research group, we prefer to use the term amphiphile to surfactant because scientists would expect surfactants to act as detergents. Detergents are often associated with

cytotoxicity, inflammation, and irritation. For this reason, it is our desire to make amphiphiles that do not act as detergents. Amphiphiles become detergents at or near the CMC[5]. Our research goal is to synthesize amphiphiles that have high CMCs and have biological activity at low concentrations of amphiphile. Having the CMC and biological activity concentrations far apart from each other will reduce the likelihood of detergency being a mechanism of action, thus reducing the probability of irritation or other unwanted side effects.

In most cases, antimicrobial activity (minimal inhibitory concentration, MIC) of a series of amphiphiles tends to increase (MIC decreases) with longer hydrocarbon chain length[6, 7]. In order to achieve high activity, one must sacrifice solubility due to the longer chain length[8]. Antimicrobial activity does not have a linear relationship with chain length. A "cutoff effect" (Figure 1.2, a generic example) is commonly observed within a homologous series of amphiphiles[6]. In this phenomenon, antimicrobial activity increases (log MIC is more negative) to a specific chain length, after which it decreases (log MIC is less negative) with longer chain length. One possible reason for this phenomenon is decreased amphiphile concentration at the site of action, due to limited amphiphile solubility.

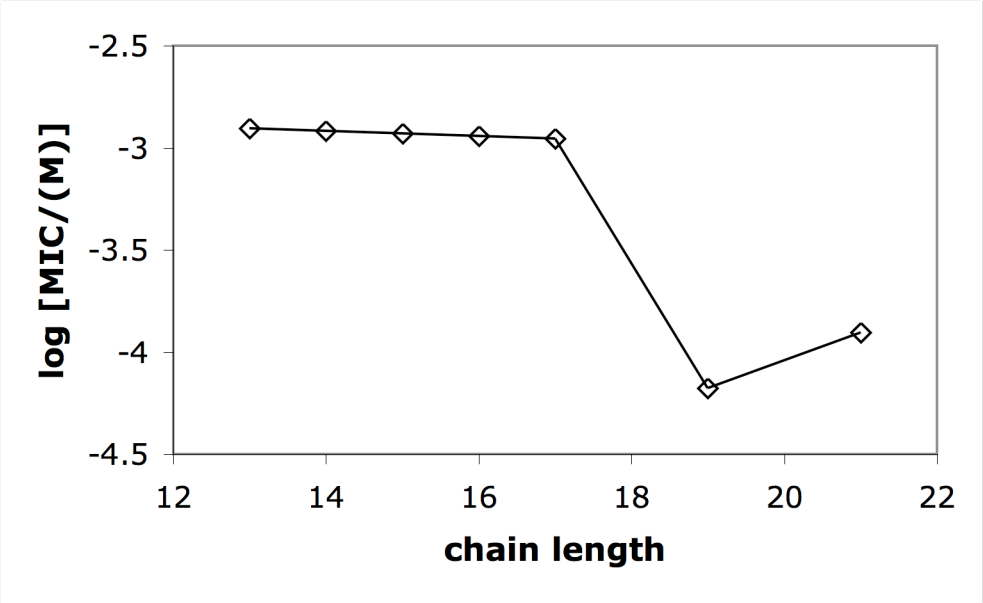

Figure 1.2 A generic example of the cutoff effect

Previous work[9] in the Gandour group has demonstrated that tri-headed anionic amphiphiles (Figure 1.3) are significantly more soluble than single-headed amphiphiles in aqueous media. This observation removes solubility as a possible cause of the "cutoff effect".

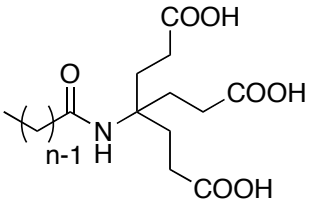

3CAmn

n = 13, 15, 17, 19, 21

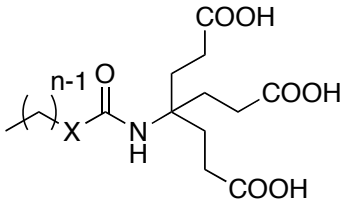

X = NH **3CUrn**
X = O **3CCbn**

n = 14, 16, 18, 20, 22

Figure 1.3 Structure of three-headed amphiphiles. Where **3C** = three carboxyl groups, **Am** = amido linker, **Ur** = urido linker, **Cb** carbamato linker, **n** = number of carbons in the tail.

The ultimate goal of this project is to synthesize topical microbicides, especially those active against *S. aureus* and MRSA. The individual goals of this research includes

(1) synthesis, and characterization of two-headed amphiphiles, (2) measurement of CMCs, and (3) measurement of antimicrobial activity (measured by Shauntrece Hardrict and Myra Williams).

1.2 Introduction to Amphiphiles

An amphiphile (Figure 1.4) is a term used to describe a molecule that has two characteristic parts: a hydrophilic group (the polar headgroup) and the hydrophobic tail (the non-polar tail). The headgroup can consist of an anionic, cationic, nonionic, and zwitterionic functional groups (Table 1.1)[10, 11].

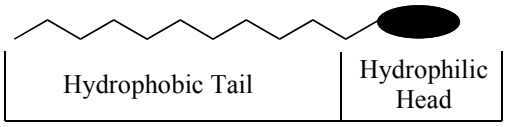

Figure 1.4 General structure of an amphiphile

The non-polar tail often consists of saturated or unsaturated hydrocarbon chains of various lengths, however, chains consisting of alkylbenzenes, alkylnaphthalenes, and branched-chain alkyl groups are also common[12]. Different variables, such as, temperature, structure, solution conditions, and counterions affect the solubility, activity, and CMC of a given amphiphile.

Table 1.1 Examples of anionic, cationic, nonionic, and zwitterionic amphiphiles

Anionic Headgroups	**General Structure R = hydrophobic tail**	**Cationic Headgroups**	**General Structure R = hydrophobic tail**
Sulfonate	$R\text{-}SO_3^-M^+$	Ammonium salts	$R_xH_yN^+X^-$
Sulfate	$R\text{-}OSO_3^-M^+$	Quaternary Ammonium Salts	$R_4N^+X^-$
Carboxylate	$R\text{-}COO^-M^+$		
Phosphate	$R\text{-}OPO_3^-M^+$		
Zwitterionic Amphiphiles		**Nonionic headgroups**	
Betaines	$R\text{-}N^+(CH_3)_2CH_2CH_2COO^-$	Polyoxyethlene (POE)	$R\text{-}CH_2CH_2(OCH_2CH_2)_nOH$
Sulfobetaines	$R\text{-}N^+(CH_3)_2CH_2CH_2SO_3^-$		

One special characteristic of amphiphiles is their ability to form aggregates called micelles or bilayers (Figure 1.5). In these aggregates, the chains interact with each other through van der Waals interactions while the polar headgroups interact with each other and water. Amphiphiles with two hydrophobic tails tend to form bilayers similar to phospholipids in cell membranes. The interiors of micelles have properties of liquid hydrocarbons and allow micelles to solubilize non-polar organic molecules that are insoluble in water. This unique property allows amphiphiles to be used as emulsifying, foaming, and cleaning agents[13].

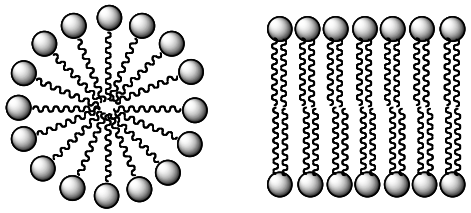

Figure 1.5 Amphiphile Aggregates

In order for an amphiphile to dissolve in water it must have a polar or ionized headgroup. From Table 1.1 we can see that the composition of the headgroup can be negatively or positively charged. Nonionized amphiphiles have an uncharged headgroup and can hydrogen bond to water. Zwitterionic amphiphiles have a combination of negative and positive changes in the headgroup, which allows the amphiphile to be cationic, or neutral depending on the pH of the solution.

The pH of a solution can have an effect on the solubility for a given amphiphile (Table 1.2)[14]. Nonionic amphiphiles are soluble over a wide pH range because they can hydrogen bond with water. Zwitterionic amphiphiles are also soluble over a wide pH range because of the anionic and cationic groups associated with the amphiphiles. Ammonium salts are soluble in acidic conditions, while the quaternary ammonium salts

are soluble over a wide range of pH due to its permanent positive charge. Anionic amphiphiles are soluble in slightly acidic to basic conditions.

Table 1.2 pH Solubility of amphiphiles

Surfactant Type	pH Solubility
Anionic	5–14
Nonionic	3–12
Ammonium Salts	1–8
Quaternary Ammonium Salts	1–14
Zwitterionic	1–6, 8–14

1.3 Aqueous Solubility

Antimicrobial activity of saturated fatty acids (FAs) as a function of chain length has been investigated since the 1920s[15]. In general the most active FAs tend to have a chain length between C_{10}–C_{14}. Longer-chain FAs (C_{16}–C_{20}) are not active towards a wide range of microorganisms. One reason for the inactivity of the longer-chain FAs is that they have low or no aqueous solubility due to the hydrophobic nature of the long-chain FAs.

To help overcome the challenges of low aqueous solubility and to better study the relationship between activity and chain length, the Gandour group has successfully designed and synthesized long-chain water-soluble amphiphiles[9, 16]. A dendritic headgroup, incorporating three carboxylic acid groups (Figure 1.3), was used to overcome solubility as a limiting factor for antimicrobial activity. A question that arose from this work was whether these three-headed amphiphiles are too water-soluble. An amphiphile that is too hydrophilic would be less likely to partition into a cell and therefore may be less active. In order to address this issue a series amphiphiles containing dicarboxylato headgroups was synthesized (Figure 1.1) to compare with the

tricarboxylato amphiphiles (Figure 1.3). Many different comparisons will be made including the correlation of CMCs to structure, MICs to chain length (**n**), calculated logarithm of the partition coefficient (clogp)[17], and logarithm of the octan-1-ol–water distribution coefficient (logD)[18].

1.4 CMCs of Multi-headed, Anionic Amphiphiles

Along with our desire that the **2CAmn** series be soluble in aqueous media, we want this series to have high CMCs, which is defined as the concentration at which amphiphiles spontaneously form micelles. This value is important to measure because it is believed that the non-detergent antimicrobial activity of amphiphiles are caused by monomers and not micelles[19].

Shinoda[20, 21] has done studies to explored the correlation between the number of headgroups and chain length to the CMC value (Figure 1.6)[20, 22]. The group observed that the CMC values for multi-headed amphiphiles were 3.5–15 time greater than those of the corresponding FA (Figure 1.7)[21]. These results were attributed to the increased repulsion of the headgroups in a micelle[21].

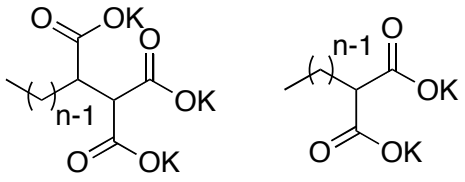

1 **2**

n = 8–18

Figure 1.6 Structures of multi-headed amphiphiles studied by Shinoda

CMC values were collected for a homologous series of dicaboxyl potassium alkyl malonates, **2**, with different chain lengths[22]. The results showed that the CMC

decreased as the length of the hydrophobic tail increases. The longer the hydrophobic tail of an amphiphile, the stronger the van der Waals interactions between molecules in a micelle. The work[20] performed also revealed that the logarithm of the CMC has a linear relationship to the chain length of the tail (Equation 1.1)(Figure 1.7), where n is the number of carbons in the tail and k_n is the slope of the line. From Figure 1.7 we can also see that the CMC values for **1** and **2** are not very different.

$$\log CMC = -k_n n + \text{const.} \qquad \text{Equation 1.1}$$

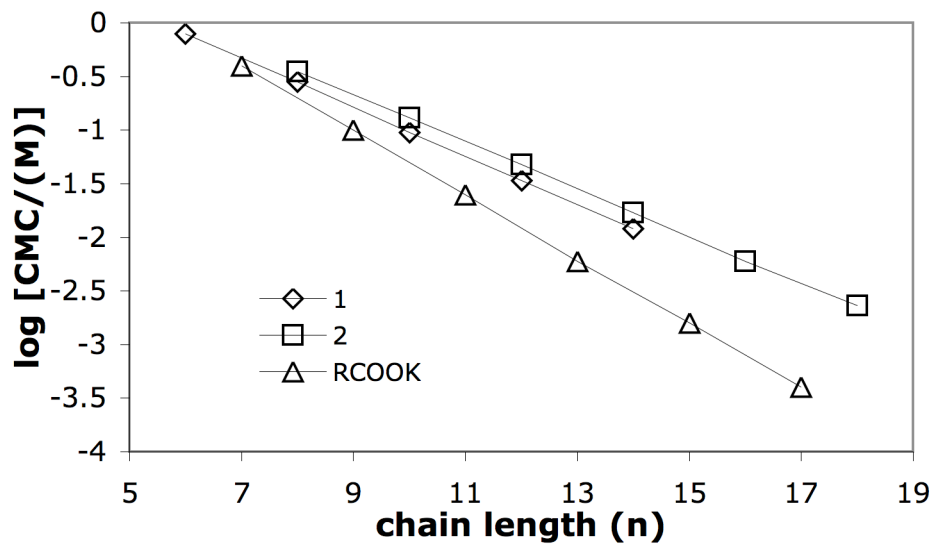

Figure 1.7 The effect of the number of headgroups on CMC

Work performed by Paleos et al.[23] explored the liquid crystal and aqueous micelle behavior of a series of iminodiacetic acid amphiphiles (Figure 1.8).

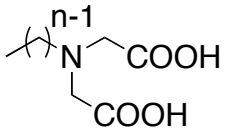

n = 12, 16, 18

Figure 1.8 Structure of iminodiacetic acid derivatives

This work[23] showed that the two-headed anionic amphiphiles have a higher CMC than the corresponding FA salt (Figure 1.9). For example, the C_{12} dianionic potassium salt has a CMC of 0.022 M while the potassium salt of the C_{12} FA has a CMC of 0.014 M. The authors[23] explain this difference by noting that the doubly charged ionic headgroup of the iminodiacetic acid derivatives makes the amphiphiles more water-soluble than the corresponding FA. Comparing the work from Shinoda[20] and Paleos et al.[23], there is no dramatic CMC difference between **2** (Figure 1.6) and the iminodiacetic acid derivatives (Figure 1.8). The author also reports[23] the aggregation numbers for the series of amphiphiles, which indicates that the micelles are not spherical and form loose micelles. This work[23] also revealed that water penetrates into the micellar palisade region. Paleos et al.[23] concludes that the bulky doubly charged ionic head on the amphiphile creates serious packing problems and leads to a loose micelle structure.

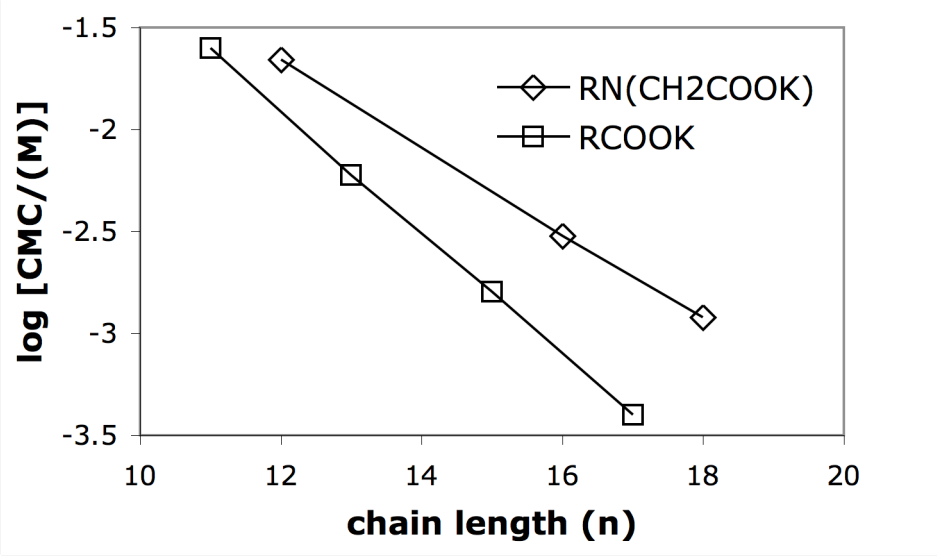

Figure 1.9 The effect of two headgroups on CMC

Previous work[16] performed by the Gandour group has shown that three-headed ionic amphiphiles (Figure 1.3) are water-soluble and have CMC values much higher than

the corresponding FAs. The work[16] also showed that these amphiphiles have CMC values ~100 times greater than the MIC. The CMC for these amphiphiles decreases with increasing chain length, which agrees with the observations made by Shinoda[22]. With this work[16] the Gandour group has been able to measure the monomeric amphiphile activity. Based on Figures 1.7 and 1.9, we hypothesize that an amphiphile with a dianionic headgroup (**2CAmn**) will have a higher CMC than the corresponding FA but slightly lower than the trianionic amphiphiles.

1.5 Introduction to *Staphylococcus aureus* and Methicillin-Resistant *Staphylococcus aureus*

Staphylococcus aureus is a Gram-positive bacterium, which causes many kinds of infections. *S. aureus* can be found colonized in the nasal cavity in about 32% of the U.S. population[24]. Nasal colonization can indicate a higher risk of subsequent infections[24]. This bacterium is the most common cause of skin and soft tissue infections resulting in 11.6 million visits for ambulatory care[25]. *S. aureus* infections can progress to more serious conditions involving muscle, bone, lungs, and heart valves[25]. The contagious nature of *S. aureus* can lead to higher infection rates among young men who have skin-to-skin contact, such as those who play sports[25]. Susceptible populations, such as infants and individuals who have undergone surgery, are undergoing dialysis, or have prosthetic devises, are some of the most at risk for *S. aureus* infections[26]. Nosocomial infections caused by *S. aureus* lead to longer hospital visits and higher healthcare costs[26]. Current treatments for *S. aureus* involve draining lesions and the use of β-lactam antimicrobial drugs[25].

Strains of *S. aureus* resistant to β-lactam antimicrobial drugs, termed methicillin-resistant *S. aureus* (MRSA), were first discovered in the 1960s[27]. Through the 1990s, MRSA was associated with infections in the healthcare arena, known as healthcare-associated MRSA[27]. Since the late 1990s community-associated MRSA has become more prevalent in persons without established healthcare risk factors[28, 29]. As with *S. aureus*, MRSA impacts persons with weakened immune systems, but it also impacts individuals who are otherwise healthy.

There are many treatments for MRSA infections, including the popular drug, vancomycin (Figure 1.10). With the increasing use of these drugs, rare strains of MRSA have been found to be susceptible only to a short list of antibiotics[30]. There are topical agents, such as mupirocin (Figure 1.10), that can be applied in the nasal cavity of those who are colonized with MRSA in an effort to prevent future infections. However, mupirocin-resistant strains have been isolated, which makes it harder to treat MRSA infections[31].

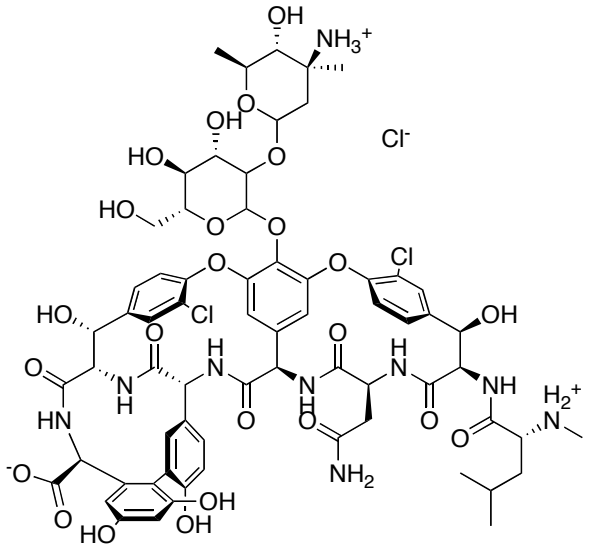

Vancomycin

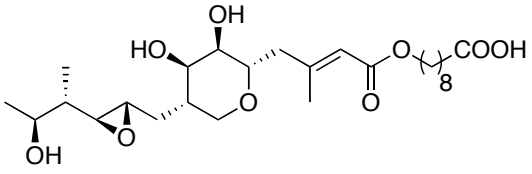

Mupirocin

Figure 1.10 Examples of drugs used to treat MRSA

1.6 Antimicrobial Activity of Fatty Acids against *S. aureus*

FAs have been known to display antimicrobial activity since the 1920s[15, 32]. Many studies have been done to observe the relationship between FAs and their activity against *S. aureus* (Table 1.3). The work[15, 33-39] summarized below shows that the most active saturated FA has a chain length between C_{12} and C_{14}. In most studies, the cutoff effect was observed with the longer-chain (> C_{14}) FA having less activity. Work performed by Ohta et al.[40] showed that unsaturated FAs were considerably more active against *S. aureus* than unsaturated FAs.

Table 1.3 Summary of FA studies on *S. aureus*

Author	Most Active Saturated FA	Notes	Reference
Walker	None	Measurements showed no activity against *S. aureus*.	[15]
Bayliss	C_{12}	Longer chain (C_{14}–C_{18}) FAs were inactive.	[33]
Kabara et al.	C_{12}; 2450 μM	The cutoff effect was observed with longer chain (C_{14}–C_{18}) FAs being less active.	[34-37]
Jossifova et al.	C_{14}; 5690 μM	The cutoff effect was observed with longer chain (C_{16}–C_{18}) FAs being less active.	[38]
Kitahara et al.	C_{14}; 1750 μM	The cutoff effect was observed with longer chain (C_{16}–C_{18}) FAs being less active.	[39]
Author	Most Active Unsaturated FA	Notes	Reference
Ohta et al.	$C_{18:3}$; 36 μM	Activity increases with the number of double bonds.	[40]

1.7 Antimicrobial Activity of Fatty Acids against MRSA

Ohta et al.[40] reported the antibacterial activity of both saturated and unsaturated FAs, against MRSA. As with the results against *S. aureus* (Table 1.3), the activity of the FAs increases with the number of double bonds. FAs with three double bonds were found to be more active than FAs with a single double bond. Oleic acid ($C_{18:1}$) was inactive, while linolenic acid ($C_{18:3}$) was active at 72 μM.

Kitahara et al.[39] studied the antibacterial activity of saturated FAs against five strains of MRSA. In all cases, antimicrobial activity increased with chain length, from C_8 (> 11 mmol) to a maximum at C_{12} (2.0 mmol). In four of the five strains, the longer-chain FAs (C_{14}–C_{18}) were mostly inactive (≥ 11 mmol).

1.8 Antimicrobial Activity of Dendritic Amphiphiles Against *S. aureus*

The Gandour group has successfully synthesized long chain (C_{13}–C_{22}) water-soluble dendritic amphiphiles[9]. The amphiphiles were tested against *S. aureus* and the results (Figure 1.11) show that in general, the activity increases (log MIC is lower) with increasing chain length. The most active amphiphile (**3CCb22**) against *S. aureus* was found to have an MIC of 333 μM. These measurements were performed at a high inoculum density [10^8 colony-forming units (CFU/mL)]. The cutoff effect was observed with **3CUrn** where **3CUr16** was the most effective while the longer chain amphiphiles were less active. The two other series (**3CAmn**, **3CCbn**) are still increasing in activity (log MIC still decreasing) with longer chain length, suggesting that ultra-long chain ($\geq C_{23}$) may be more active.

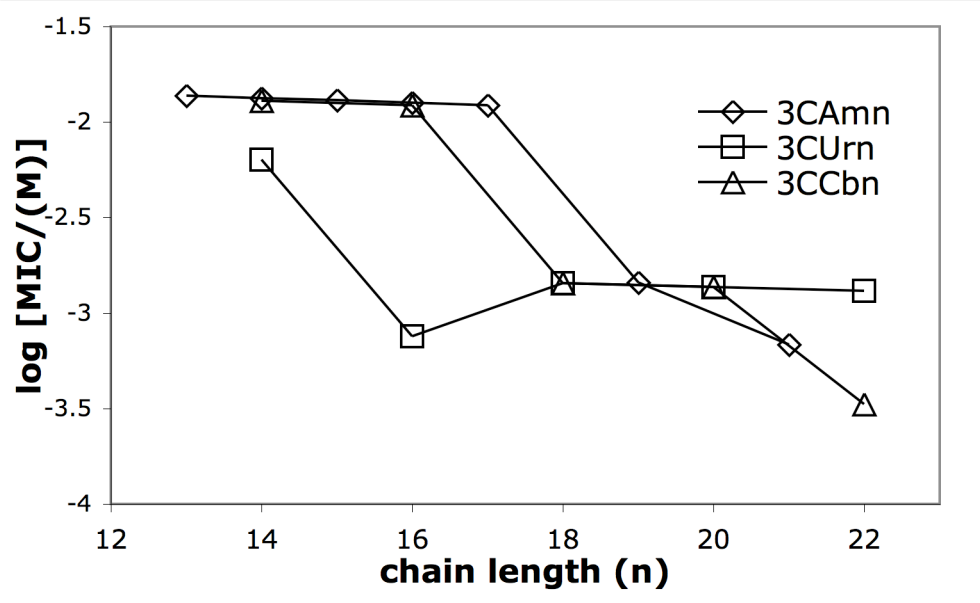

Figure 1.11 *S. aureus* MICs for three-headed amphiphiles at high inoculum density

These results[9] demonstrate that very long chain (≥ 20 carbons) water-soluble amphiphiles are much more active than FAs against *S. aureus*.

1.9 Antimicrobial Activity of Dendritic Amphiphiles Against MRSA

The same sets of compounds used in Section 1.8 were used to measure the antimicrobial activity against MRSA[9]. As with the results against *S. aureus*, activity generally increased with chain length to a maximum MIC of 64 μM for **3CAm19** (Figure 1.12). The cutoff effect was observed with **3CAmn** and **3CUrn** while **3CUrn** is still increasing in activity with chain length. These measurements were performed at a high inoculum density [10^8 colony-forming units (CFU/mL)].

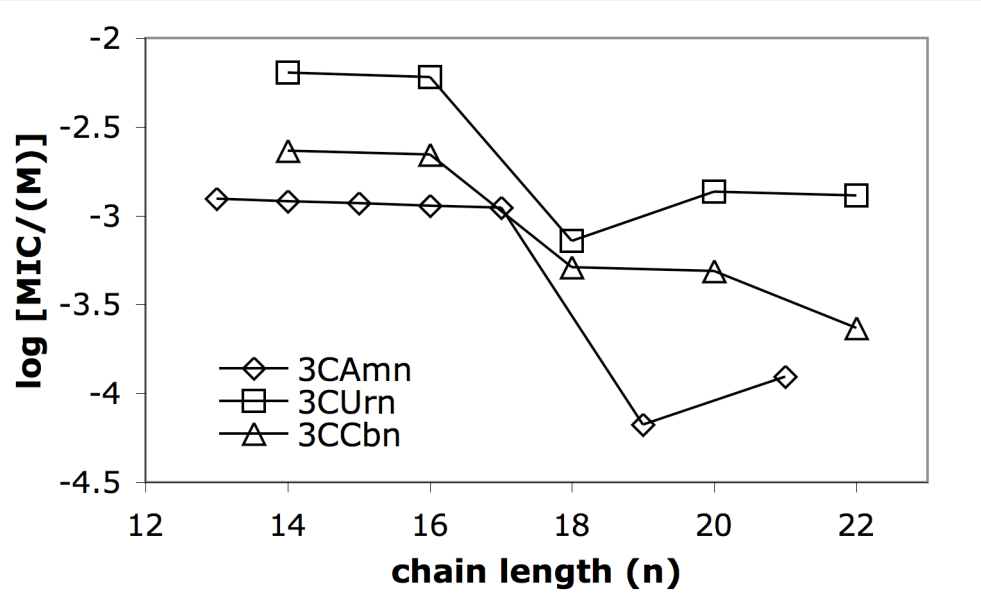

Figure 1.12 MRSA MICs for three-headed amphiphiles at high inoculum density

1.10 Conclusion

Overall, the three-headed amphiphiles (Figure 1.3) have been shown to be water-soluble, have high CMCs relative to the MIC, and have antimicrobial activity[9, 16]. From this work we would expect that the **2CAmn** series would be water-soluble, have higher CMCs than the corresponding FA and lower CMCs than the corresponding homologues in the **3CAmn** series, and have antimicrobial activity against *S. aureus* and MRSA.

1.11 References for Chapter 1

1. Cross, J., *Surfactant Science*, ed. S. J. Cross, E. J. Vol. 53. 1994, New York: Marcel Dekker. 7-14.
2. Urizzi, P., Souchhard, J. P., Nepvue, F., *EDTA and DTPA analogs of dipalmitoylphosphatidylethanolamine as lipophilic chelating agents for metal labeling of LDL.* Tetrahedron Lett., 1996. **37**: p. 4685-4688.
3. Lawrence, C.A., *Surfactant Science*, ed. E.E. Jungermann. Vol. 4. 1970, New York: Marcel Dekker. 491-495.
4. Myers, D., *Surfactant Science and Technology*. 1988, New York, N. Y.: VCH. p. 65.

5. Dennis, E.A., *Micellization and solubilization of phospholipids by surfactants.* Adv. Colloid Interface Sci., 1986. **26**: p. 155-175.
6. Balgavy, P., Devinsky, F., *Cut-off effect in biological activities of surfactants.* Adv. Colloid Interface Sci., 1996. **66**: p. 23-63.
7. Devinsky, F.A., Sersen, F., Balgavy, P., *Interaction of surfactant with model and biological membranes. Part VIII. Cut-off effect in antimicrobial activity and in membrane perturbation efficiency of the homologous series of N,N-dimethylalkylamine oxides.* J. Pharm. Pharmacol., 1990. **42**(11): p. 790-794.
8. Klevens, H.B., *Solubilization.* Chem. Rev., 1950. **47**: p. 1-74.
9. Williams, A.A., Sugandhi, E. K., Macri, R. V., Falkinham III, J. O., Gandour, R. D., *Antimicrobial activity of long-chain, water-soluble, dendritic tricarboxylato amphiphiles.* J. Antimicob. Chemother., 2007. **59**: p. 451-458.
10. Clint, J.H., *Surfactant Aggregation*. 1991, New York: Chapman and Hall. p. 5.
11. Myers, D., *Surfactant Science and Technology*. 1988, New York, N.Y.: VCH. p. 33.
12. Myers, D., *Surfactant Science and Technology*. 1988, New York, N.Y.: VCH. p. 34-65.
13. Hartley, G.S., *Aqueous solutions of paraffin-chain salts; a study in micelle formation*. 1936, Paris: Hermann & C. 42-45.
14. Lomax, E.G., *Amphoteric Surfactant*. 2nd ed, ed. E.G. Lomax. 1996, New York: Marcel Dekker Inc. p. 3.
15. Walker, J.E., *The germicidal properties of chemically pure soaps.* J. Infect. Dis., 1924. **35**: p. 557-566.
16. Sugandhi, E.K., Macri, R. V., Williams, A. A., Kite, B. L., Slebodnick, C., Falkinham, J. O. III, Esker, A. R., Gandour, R. D., *Synthesis, critical micelle concentration, and antimycobacterial properties of homologous dendritic amphiphiles. Probing intrinsic activity and the "cutoff" effect.* J. Med. Chem., 2007. **50**: p. 1645-1650.
17. *Marvin Sketch 5.0.0. pKa, logP, and logD calculator*. ChemAxon [cited February 1, 2008]; Available from: http://intro.bio.umb.edu/111-112/OLLM/111F98/newclogp.html.
18. Sherrer, R.A., Howard, S. M., *Use of distribution coefficients in quantitative structure-activity relationships.* J. Med. Chem., 1977. **20**: p. 53-58.
19. Miller, R.D., Brown, K. E., Morse, S. A., *Inhibitory action of fatty-acids on growth of neisseria-gonorrhoeae.* Infect. Immun., 1977. **17**(2): p. 303-312.
20. Shinoda, K., *The critical micelle concentrations in aqueous solutions of potassium alkyl malonates.* J. Phys. Chem., 1955. **59**: p. 432-435.
21. Shinoda, K., *The critical micelle concentration in aqueous solutions of potassium alkane tricarboxylates.* J. Phys. Chem., 1956. **60**: p. 1439-1441.
22. Shinoda, K., *The effect of alcohols on the critical micelle concentration of fatty acid soaps and the critical micelle concentration of soap mixtures.* J. Phys. Chem., 1954. **58**: p. 1136-1141.
23. Paleos, C.M., Michas, J., Malliaris, A., *Alkyl derivatives of iminodiacetic acid: A novel class of compounds forming thermotropic liquid crystals and aqueous micelles.* Mil. Cryst. Liq. Cryst., 1990. **186**: p. 251-260.

24. Kuehnert, M.J., Kruszon-Moran, D., Hill, H. A., McQuillan, G., McAllister, S. K., Fosheim, G., McDougal, L. K., Chaitram, J., Jensen, B., Fridkin, S. K., Killgore, G., Tenover, F. C., *Prevalence of staphylococcus auresus nasal colonization in the united states, 2001-2002.* J. Infect. Dis., 2006. **193**: p. 172-179.
25. McCaig, L.F., McDonald, L. C., Mandal, S., Jernigant, D. B., *Staphylococcus aureus-associated skin and soft tissue infections in ambulatory care.* Emerg. Infect. Dis., 2006. **12**(11): p. 1715-1723.
26. Talbot, G.H., Bradley, J., Edwards, Jr., J. E., Gilbert, D., Scheld, M., Bartlett, J. G., *Bad bugs need drugs: an update on the development pipeline from the antimicrobial availability task force of the infectious diseases society of America.* Clin. Infect. Dis., 2006. **42**: p. 657-668.
27. Panlilio, A.L., Culver, D. H., Gaynes, R. P., Banerjee, S., Henderson, T. S., Tolson, J. S., *Methicillin-resistant Staphylococcus aureus in u.s. hospitals, 1975–1991.* Infect. Control Hosp. Epidemiol., 1992. **13**: p. 582-586.
28. *Centers for disease control and prevention. Four pediatric deaths from community-acquired methicillin-resistant staphylococcus aureus—Minnesota and North Dakota, 1997–1999.* JAMA, 1999. **282**: p. 1123-1125.
29. Chambers, H.F., *The changing epidemiology of Staphylococcus aureus?* Emerg. Infect. Dis., 2001. **7**: p. 178-182.
30. Fridkin, S.K., Hagerman, J., McDougal, L. K., *Epidemiological and microbiological characterization of infections caused by staphylococcus aureus with reduced susceptibility to vancomycin, united states, 1997–2001.* Clin. Infect. Dis., 2003. **36**: p. 429-439.
31. Walker, E.S., Vasquez, J. E., Dula, R., Bullock, H., Sarubbi, F. A., *Mupirocin-resistant, methicillin-resistant staphylococcus aureus: does mupirocin remain effective?* Infect. Control Hosp. Epidemiol., 2003. **24**: p. 342-346.
32. Nieman, C., *Influence of trace amounts of fatty acids on the growth of microorganisms.* Bacteriol. Rev., 1954. **18**: p. 147-163.
33. Bayliss, M., *Effect of the chemical constitution of soaps upon their germicidal properties.* J. Bacteriol, 1936. **31**: p. 489-504.
34. Kabara, J.J., *Lipids as host-resistance factors of human-milk.* Nutr. Rev., 1980. **38**(2): p. 65-73.
35. Kabara, J.J., Vrable, R., Liekenjie, M. S. F., *Antimicrobial lipids -natural and synthetic fatty-acids and monoglycerides.* Lipids, 1977. **12**(9): p. 753-759.
36. Kabara, J.J., *Toxicological, bacteriocidal and fungicidal properties of fatty acids and some derivatives.* J. Am. Oil Chem. Soc., 1979. **56**(11): p. 760A-767A.
37. Kabara, J.J., *Structure-function relationship of anti-microbial lipids - Review.* J. Am. Oil Chem. Soc., 1978. **55**(3): p. A235-A235.
38. Jossifova, L.T., Manolov, I., Golovinsky, E., V., *Antibacterial action of some saturated and unsaturated long-chain carboxylic acids and their bis(2-chloroethyl)aminoethyl esters in vitro.* Die Pharmazie, 1989. **44**(12): p. 854-856.
39. Kitahara, T., Koyama, N., Matsuda, J., Aoyama, Y., Hirakata, Y., Kamihira, S., Kohno, S., Nakashima, M., Sasaki, H., *Antimicrobial activity of saturated fatty acids and fatty amines against methecillin-resistant staphylococcus aureus.* Biol. Pharm. Bull., 2004. **27**(9): p. 1321-1326.

40. Ohta, S., Shiomi, Y., Kawashima, A., Aozasa, O., Nakao, T., Nagate, T., Kitamura, K., Miyata, H., *Antibiotic effect of linolenic acid from chlorococcum strains Hs-101 and dunaliella-primolecta on methicillin-resistant staphylococcus aureus.* J. Appl. Phycol., 1995. **7**(2): p. 121-127.

Chapter 2: Synthesis of the 2CAmn Series

2.1 Introduction

The synthesis of the **2CAmn** series can be accomplished in four steps as shown in the retrosynthetic analysis (Scheme 2.1). The first step involves a reaction of nitroethane and two equivalents of *tert*-butyl acrylate to create the nitrodiester synthon **1** by successive Michael additions. The second step in the synthesis consists of a reduction of **1** to the diesteramine **2**. The third step is the condensation of an acid chloride with **2** to give an alkanamido diester (**2EAmn**). The resulting compounds are abbreviated as **2EAmn**, where "**2E**" represents two *tert*-butyl ester groups, "**Am**" represents the amido linker, and "**n**" represents the number of carbons in the hydrophobic tail. The final step is the removal of the *tert*-butyl protecting groups to give **2CAmn**. "**2C**" represents two carboxylic acid or carboxylate headgroups, "**Am**" represents the amido linker, and "**n**" represents the number of carbons in the hydrophobic tail.

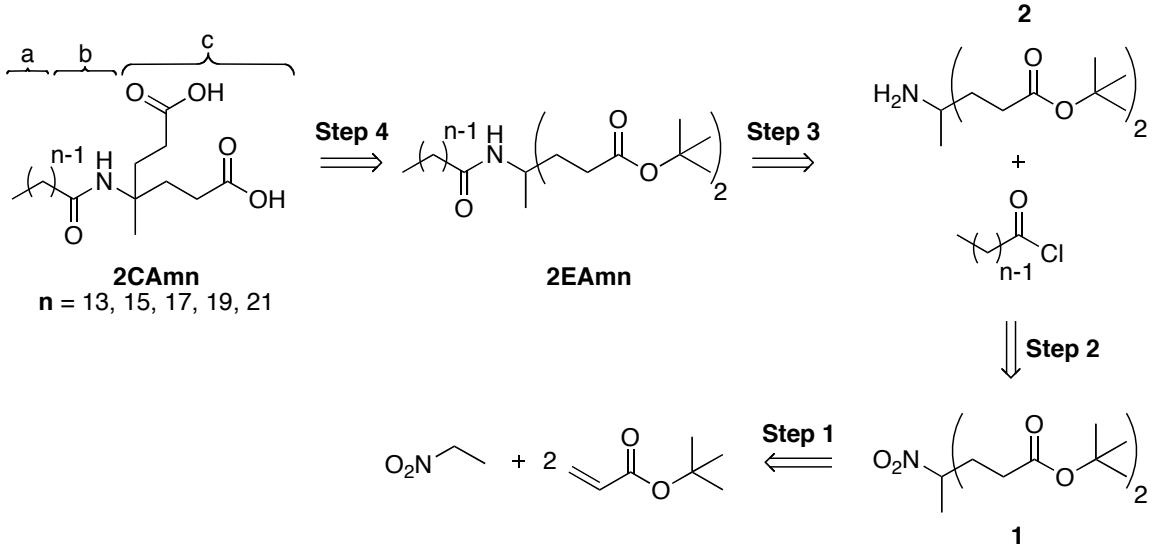

Scheme 2.1 Retrosynthesis of the **2CAmn** series. a: hydrophobic moiety; b: amido linker; c: hydrophilic moiety.

2.2 Formation of Nitrodiester

Newkome has published several methods for preparing dendritic headgroups with two *tert*-butyl ester groups (Scheme 2.2)[1, 2].

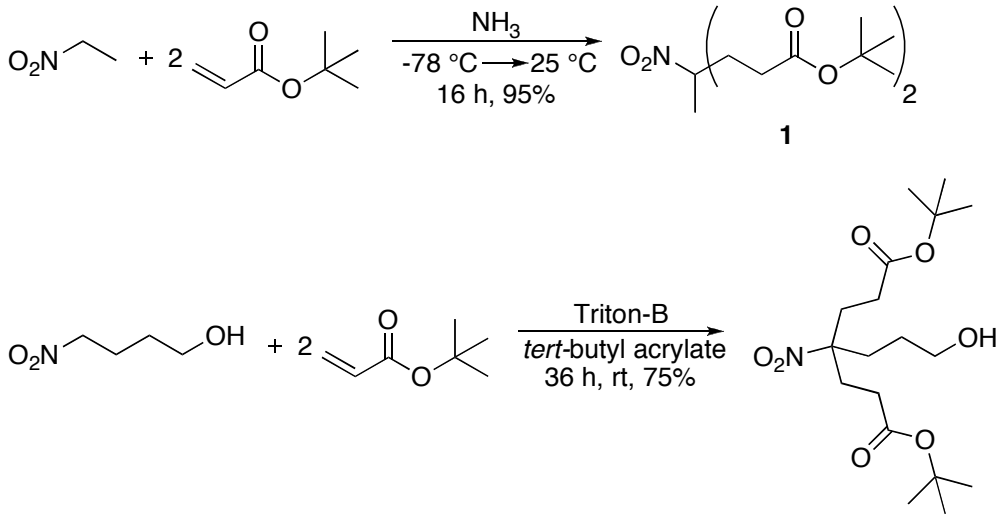

Scheme 2.2 Published methods for preparing di-*tert*-butyl ester synthons

In an effort to avoid using liquid NH_3, formation of **1** was accomplished by a reaction of nitroethane and two equivalents of *tert*-butyl acrylate by successive Michael additions using Triton B (benzyltrimethylammonium hydroxide) as a catalyst (Scheme 2.3). The reaction was run using a two-fold excess (4 equivalents) *tert*-butyl acrylate. A challenge with this procedure is the removal of the excess *tert*-butyl acrylate, which has a boiling point of 121 °C. Excess *tert*-butyl acylate was removed by bulb-to-bulb distillation. After aqueous workup, the solid was purified by recrystallizing from methanol. The white solid had a sharp melting range (higher than published[1]) and the ^{1}H NMR spectrum agreed with that published[1].

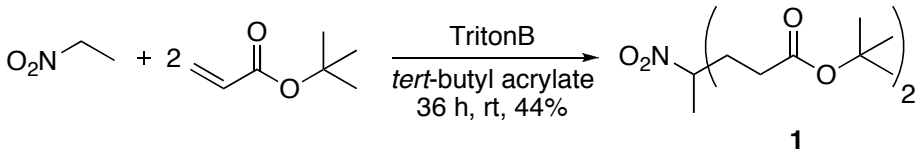

1

Scheme 2.3 Formation of nitrodiester using triton-B

To improve the yield, we also explored DBU (1,8-Diazabicyclo[5.4.0]undec-7-ene) as a catalyst for the Michael addition reaction (Scheme 2.4a)[3]. DBU worked well in the preparation of **1** while using only a small excess (2.05 equivalents) of *tert*-butyl acrylate (Scheme 2.4b). Yields were higher than the Triton-B procedure (Scheme 2.3).

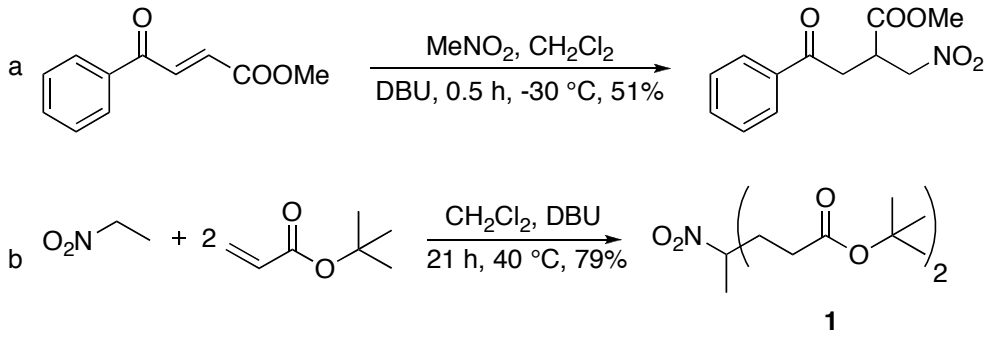

1

Scheme 2.4 Michael additions using DBU. a. Reported method using DBU. b. Current work using DBU

2.3 Formation of Diesteramine

Formation of **2** was accomplished by Newkome et al.[4] via catalytic hydrogenation of **1** (Scheme 2.5). Newkome states that a *tert*-butyl ester is needed, instead of a less bulky alkyl group to prevent intramolecular cyclization, i.e. the formation of a cyclic lactam **3**[4](Scheme 2.6). Typically, the reaction is run in an alcoholic solvent.

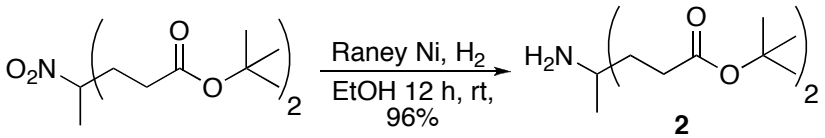

Scheme 2.5 Method for the formation of diesteramine used by Newkome

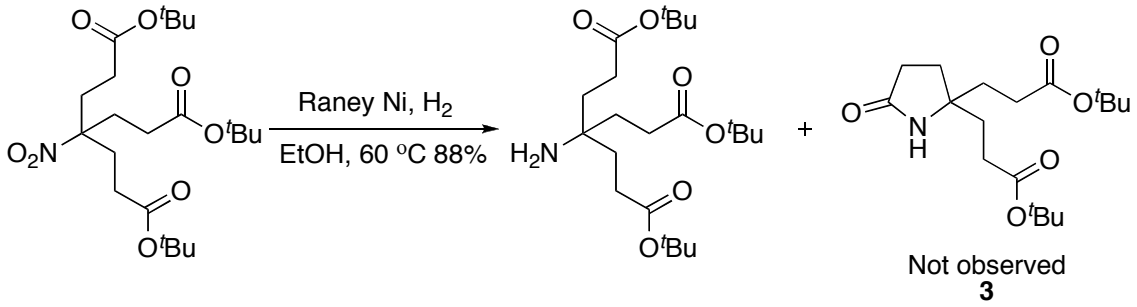

Scheme 2.6 The use of *tert*-butyl groups to prevent lactam formation

The synthesis of **2** was accomplished by modifying the method in Scheme 2.5 and allowing the reaction to proceed for only 4 h (Scheme 2.7). The white low-melting solid gave a ^{1}H NMR spectrum that agreed with that published for **2**, reported as an oil[1].

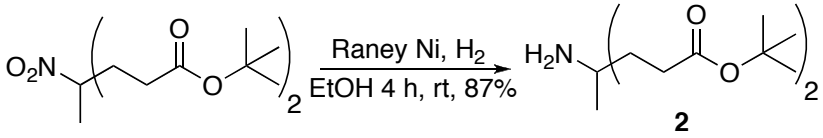

Scheme 2.7 Method used to prepare diesteramine

An alternative method for the reduction of **1** has been reported by Akpo et al.[5] using heptane instead of ethanol (Scheme 2.8), which resulted in a product with higher purity and yield (98%) compared to Newkome[4] (88%). The hydrogenation was carried out in a stirred sealed container, which the Gandour group has no access to. An attempt to run the reaction with shaking but no stirring failed to produce **2**.

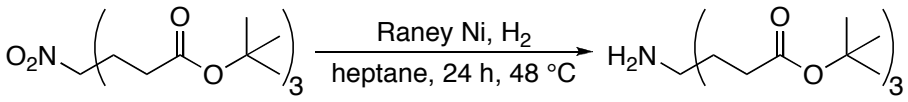

Scheme 2.8 Reduction procedure using heptane

2.4 Synthesis of Long-Chain Acid Chlorides

Acid chlorides were prepared with a modified procedure[6] by combining the appropriate fatty acid with excess thionyl chloride at ambient or elevated temperatures, which were required to dissolve the fatty acid (Scheme 2.9). The acid chlorides were collected by evaporative removal of excess thionyl chloride with chase solvents to yield oils or solids, which were > 95% pure by ^{1}H NMR analysis. The major impurities are the acids and acid anhydrides.

Scheme 2.9 Preparation of long-chain acid chlorides

2.5 Formation of an Amide Bond Utilizing Diesteramine

To obtain the **2EAmn** series, an attachment between the hydrophobic and hydrophilic moieties must be made via an amide bond (Scheme 2.1). Newkome et al.[4] employed a procedure in which a dendritic amine was allowed to react with an acid chloride. The Gandour group also used this method to develop similar amphiphiles (Scheme 2.10a)[7, 8]. To prepare **2EAmn**, diesteramine **2** was allowed to react with a long-chain acid chloride (Scheme 2.10b). The isolated solids were purified by chromatography or recrystallization and were fully characterized. Compound **2EAm17** was purified by recrystallizing from acetonitrile (35%) and the other esters (**2EAm13**, **2EAm15**, **2EAm19**, **2EAm21**) were purified by flash chromatography (76–78%).

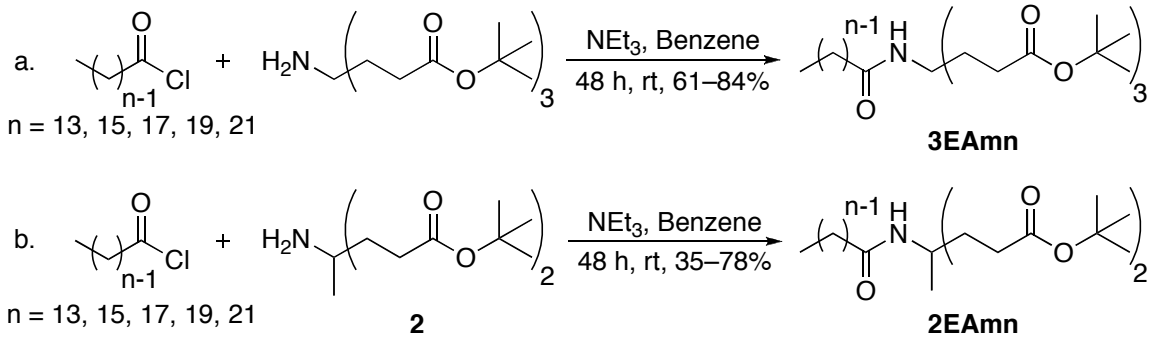

Scheme 2.10 Synthetic route for the preparation of **2EAmn**. a. Developed method used for the preparation of **3EAmn**. a. Synthetic method used for the preparation of **2EAmn**.

2.6 Removal of the *tert*-Butyl Groups via two Methods

tert-Butyl groups are routinely removed under acidic conditions with formic acid or trifluoroacetic acid (TFA) (Table 2.1)[2, 9-11]. Newkome utilized formic acid to remove the *tert*-butyl groups of various dendritic polymers or dendrons[4, 12-14] (not shown). Others[9-11] used trifluoroacetic acid to remove *tert*-butyl groups from various compounds(Table 2.1)[9].

Table 2.1 Removal of *tert*-butyl groups via two methods

Deprotected Product	Reaction Conditions	Ref.
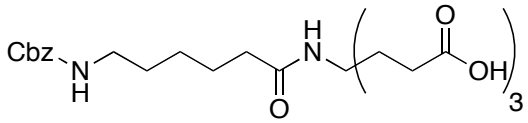	CF_3COOH, CH_2Cl_2, 2 h, 88%	[9]
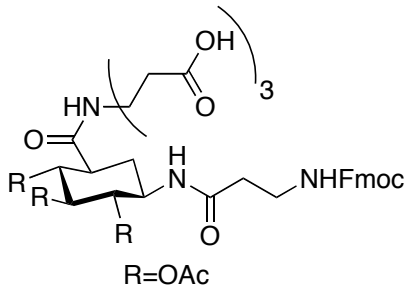	CF_3COOH, $C_2H_4Cl_2$, rt, 3 h, 79%	[11]
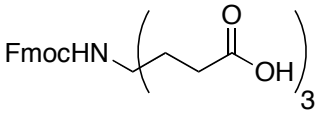	CF_3COOH, $C_2H_4Cl_2$, 1 h, 62%	[10]
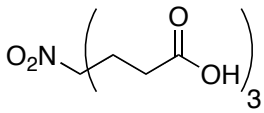	HCO_2H, 4 h, 25 °C	[2]

Both the formic acid and a modified TFA procedure were used to remove the *tert*-butyl groups from **2EAmn** (Scheme 2.11). The TFA procedure is preferred due to the short duration of the reaction. The white solids were purified by recrystallization from either acetic acid or ethanol and were fully characterized.

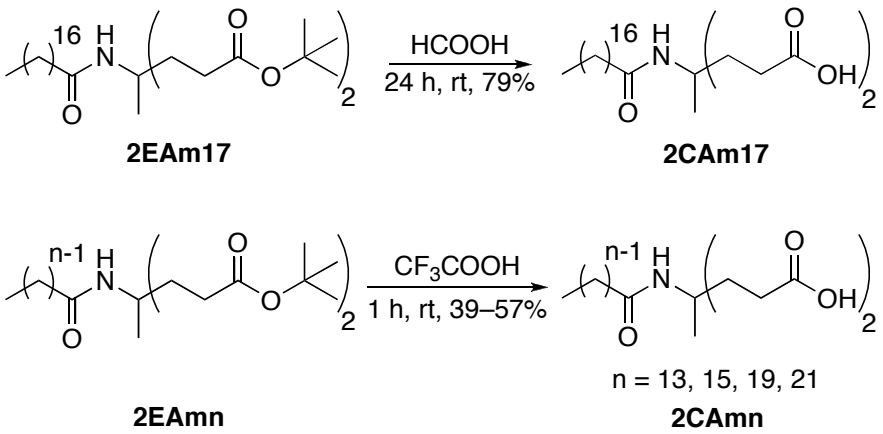

Scheme 2.11 Removal of the *tert*-butyl group

2.7 Overall Synthesis of the 2CAmn Series

Four steps are needed to form the **2CAmn** series (Scheme 2.12). The first step is the formation of nitrodiester via successive Michael additions then a reduction to the diesteramine. The third step is a condensation reaction to yield **2EAmn** followed by the removal of the *tert*-butyl groups to produce **2CAmn**. It is important to note that none of the reactions below have been optimized. Higher yields would be expected with optimized reactions and improved purification techniques.

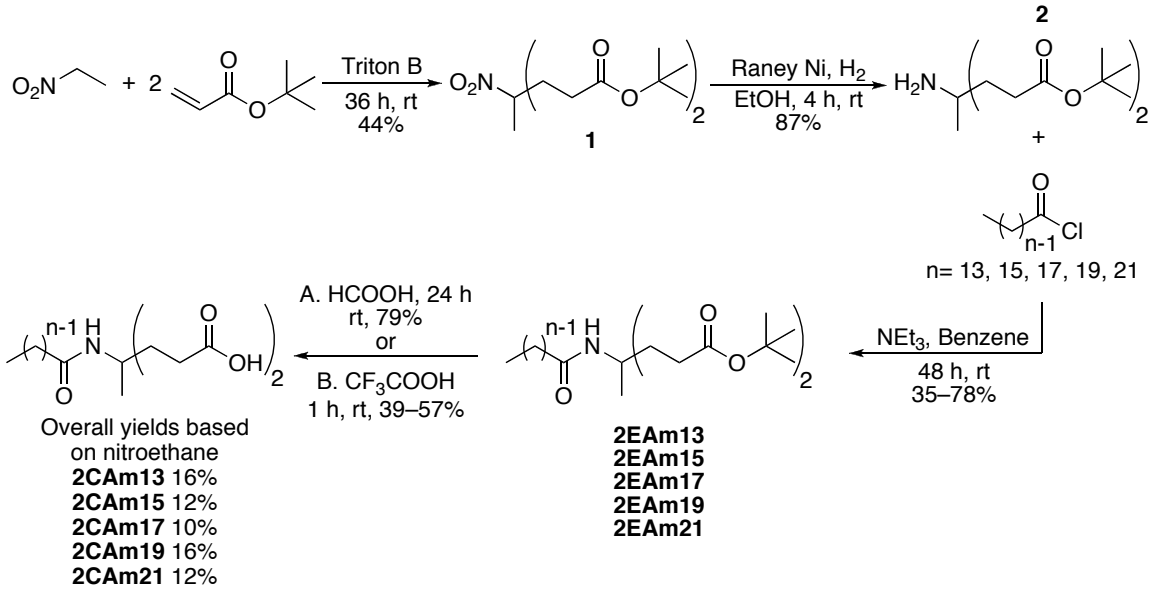

Scheme 2.12 Synthesis scheme for the **2CAmn** series

2.8 Comment on NMR Characterization: Diastereotopic Protons

We were initially surprised with the complexity of the ^{1}H NMR spectrum for the two-headed compounds compared to the three-headed counterparts. The ^{1}H NMR spectra of nitrodiester (Figure 2.1, left), displayed complex splitting for the eight methylene protons.

This phenomenon can be explained by looking at the environment surrounding the protons. Figure 2.2 is a three-dimensional representation of nitrodiester and nitrotriester. As there is no mirror plane for nitrodiester which would allow for H_a to reflect onto $H_{a'}$, or H_b to reflect onto $H_{b'}$, the protons are in different chemical environments. However, there is one mirror plane, which allows for one headgroup to reflect onto the other (Figure 2.2). If one of the methylene protons were replaced with another atom, the resulting compound would have two chiral centers, making these protons diastereotopic. Each methylene proton would be expected to have a ddd splitting pattern, resulting in a total of 32 lines for all eight protons. The mirror plane in

nitrotriester allows H_a to reflect onto H_a, and H_b to reflect onto H_b. These protons are not diastereotopic and a simple splitting pattern is observed (Figure 2.1, right).

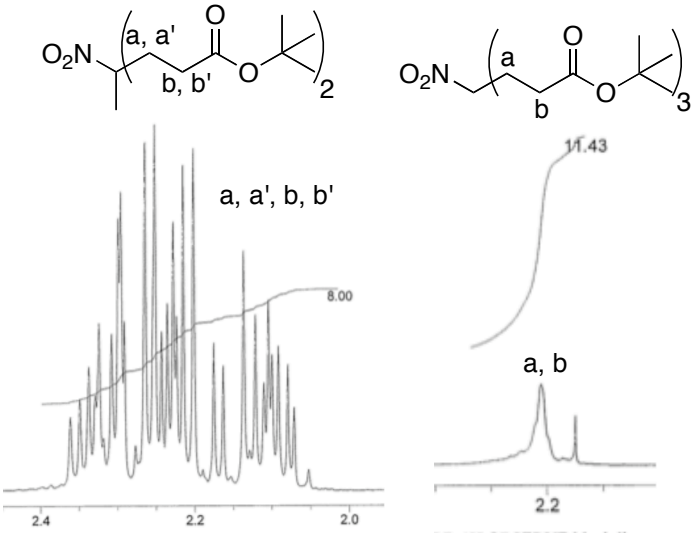

Figure 2.1 ^{1}H NMR spectra for nitrodiester and nitrotriester

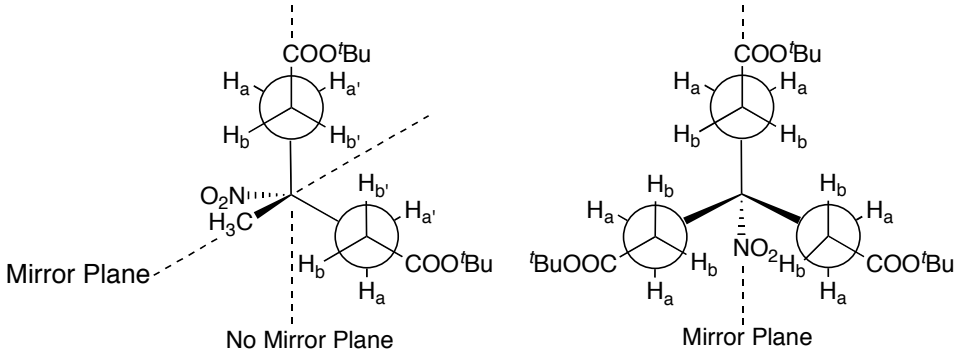

Figure 2.2 Three-dimensional representation of nitrodiester and nitrotriester.

The complex diastereopic proton splitting is observed throughout the synthesis of **2CAmn**. Diesteramine (Figure 2.3, left) shows a similar splitting pattern to triesteramine (Figure 2.3, right). Complex splitting patterns are also observed for **2EAmn** (Figure 2.4, left) and **2CAmn** (Figure 2.4, right).

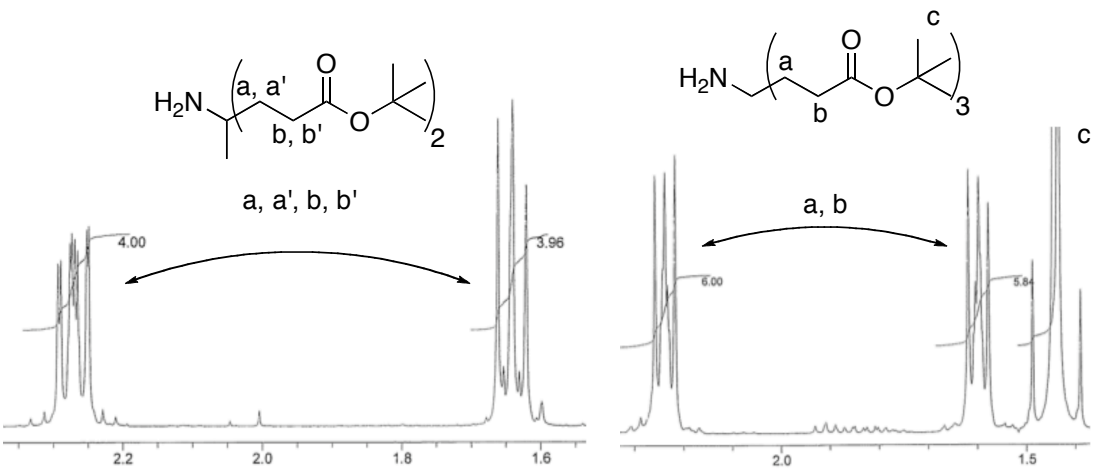

Figure 2.3 ^{1}H NMR spectra for diesteramine and triesteramine

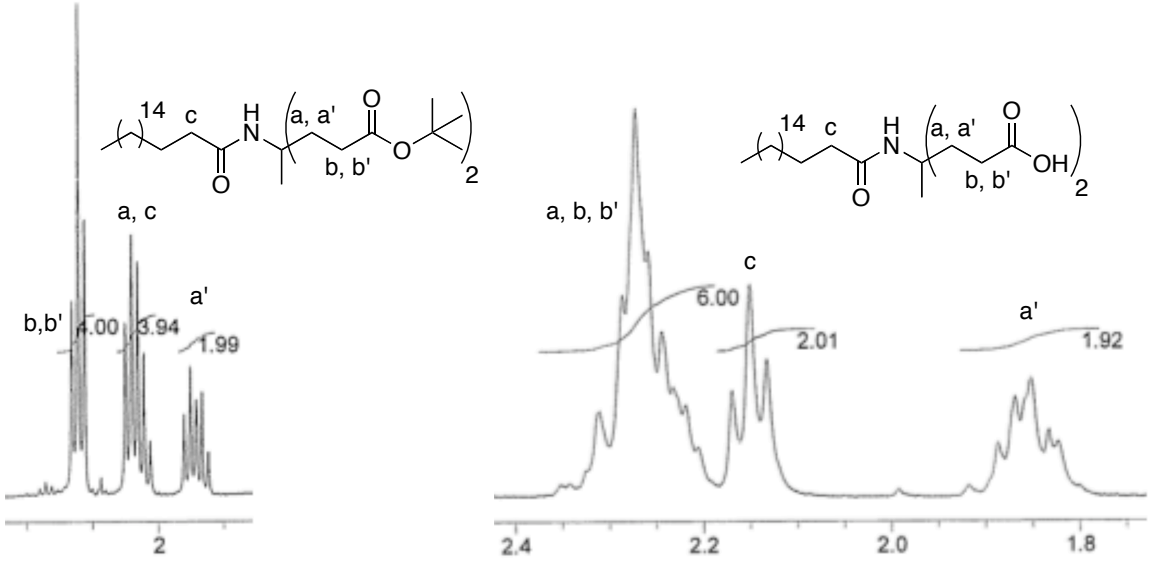

Figure 2.4 ^{1}H NMR spectra of **2EAm17** and **2CAm17**

2.9 General Comments for Synthetic Work

Unless specified, solvents and reagents were used as received. Benzene was dried with 4 Å molecular sieves. Analytical thin layer chromatography was performed on plastic-coated silica gel 60 Å and detected by dipping in a solution of 5% ethanolic phosphomolybdic acid reagent (20 wt. % solution in ethanol) and then heated with a heat gun for ~1 min. The R_f for a given **2EAmn** ranged from 0.3–0.5; the compounds were eluted in the following solvent mixtures—**2EAm13**, hexanes:ethyl acetate (4:1 vol:vol);

2EAm15, hexanes:ethyl acetate (3:1 vol:vol); **2EAm19**, hexanes:ethyl acetate (8.5:1.5 vol:vol); **2EAm21**, chloroform:ethyl acetate (9.5:0.5 vol:vol). Preparative flash column chromatography was carried out on silica gel (60 Å). After eluting the solvent mixture (100 mL), fractions (35 mL) were collected. The flow rate (~23 mL/min) was controlled by compressed air. The product appeared in fractions 3 to 12. Solutions were concentrated by rotary evaporation. Melting points were determined in open capillary tubes at 1 °C/min and uncorrected. NMR spectra of **2CAmn** series were recorded at 400 and 100 MHz for ^{1}H and ^{13}C, respectively, and reported in ppm. IR spectra were recorded on neat samples with an FTIR equipped with a diamond ATR system, and reported in cm^{-1}. HRMS data were obtained on a dual-sector mass spectrometer in FAB mode with 2-nitrobenzylalcohol as the proton donor. Elemental analyses were performed by a commercial vendor.

2.10 Experimental Procedure for the Formation of Di-*tert*-butyl 4-Methyl-4-nitroheptanedioate, Nitrodiester. Triton-B Procedure.

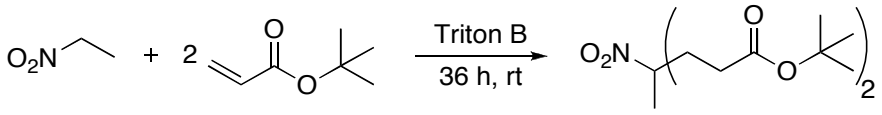

TritonB (benzyltrimethylammonium hydroxide, 8.0 mL, 40 w % solution in MeOH, 18 mmol) was added to a solution of nitroethane (25.63 g, 0.341 mol) and *tert*-butyl acrylate (164.27 g, 1.28 mol) in 5 drop portions every 15 min for the first 45 min. After 45 min the remaining Triton B was added over 5 min and allowed to react for 36 h at 25 °C yielding a brown solution. The solution was placed on a Kugelrohr distillation apparatus for 1 h at 120 °C to remove *tert*-butyl acrylate, the reduced liquid was set aside overnight. The dark brown liquid solidified to a mushy consistency (122.70 g) which

was dissolved in diethyl ether (100 mL) and washed with 5% aq HCl (1 × 100 mL), H_2O (1 × 100 mL), saturated $NaHCO_3$ (1 × 100 mL), saturated NaCl (1 × 100 mL), and dried with $MgSO_4$. The brown liquid was concentrated and recrystallized three times from methanol to yield a white solid, which was dried under high vacuum for 24 h (50.03 g, 0.442 mol, 44.2%): mp 52.5–53.3 °C; ^{1}H NMR δ ($CDCl_3$) 1.44 (s, 18H), 1.53 (s, 3H), 2.1–2.4 (m, 8H); literature[1] mp 46–47 °C; ^{1}H NMR δ 1.36 (s, 18H), 1.51 (s, 3H), 2.00–2.45 (m, 8H).

2.11 Experimental Procedure for the Formation of Di-*tert*-butyl 4-Methyl-4-nitroheptanedioate, Nitrodiester. DBU Procedure.

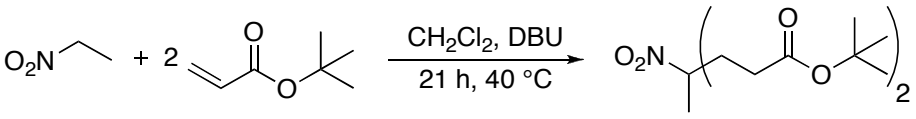

DBU (0.4 mL, 2.67 mmol) was added in 0.05 mL portions every 10 min to a stirring solution of nitroethane (4.04 g, 53.8 mmol) and *tert*-butyl acrylate (14.2 g, 111 mmol) in dichloromethane (52 mL) at 40 °C. The brown solution was stirred for 21 h. The reaction mixture was concentrated resulting in a green solid, which was dried under high vacuum for 24 h (16.8 g, 94%). The green solid (9.98 g) was purified by flash chromatography with silica gel (560 g, 28 × 7.2 cm column, $CHCl_3$:EtOAc 97.5:2.5 vol:vol) to produce a white solid (8.31 g, 25.1 mmol, 79% overall yield): mp 47.5–49.3 °C; ^{1}H NMR δ ($CDCl_3$) 1.44 (s, 18H), 1.53 (s, 3H), 2.1–2.4 (m, 8H); literature[1] mp 46–47 °C; ^{1}H NMR δ 1.36 (s, 18H), 1.51 (s, 3H), 2.00–2.45 (m, 8H)

2.12 Experimental Procedure for the Formation of Di-*tert*-butyl 4-Amino-4-methylheptanedioate, Diesteramine

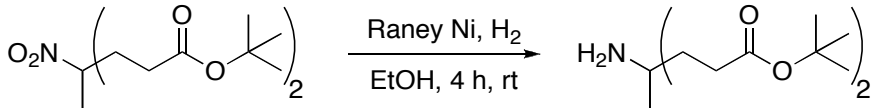

A solution of nitrodiester (4.03 g, 12.2 mmol) in 95% EtOH (30 mL) was added to Raney Ni (2.79 g, 50:50 slurry in water, 23.8 mmol). The reaction mixture was shaken in a sealed container under H_2 (56 psi) for 4 h at 25 °C, the mixture was then filtered cautiously through Celite® to remove the catalyst. The filtrate was concentrated at rt and dried under high vacuum for 48 h to afford a white solid (3.17 g, 86.6%): mp 30–31 °C; ^{1}H NMR ($CDCl_3$) δ 1.03 (s, 3H), 1.25 (s, 2H), 1.44 (s, 18H), 1.64 (m, 4H), 2.27 (m, 4H); literature[1] ^{1}H NMR ($CDCl_3$) δ 1.10 (s, 2H), 1.38 (s, 3H), 1.52 (s, 18H), 1.75 (m, 4H), 2.27 (m, 4H). This material was used immediately in the next step.

2.13 Experimental Procedure for the Formation of Tetradecanoyl Chloride

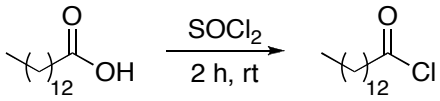

A solution of tetradecanoic acid (3.8277 g, 16.8 mmol) and thionyl chloride (35 mL) was allowed to stir for 2 h at rt. The reaction mixture was concentrated, then a chase solvent was added and the mixture was re-concentrated. This was performed four times, first using toluene (2 × 30 mL) and then dichloromethane (2 × 30 mL). The light brown oil was dried under high vacuum for 24 h. The resulting light brown oil (4.1271 g, 16.7 mmol, 99%) was used in the next step without further purification: ^{1}H NMR ($CDCl_3$) δ 0.88 (t, 3H), 1.26 (m, 20H), 1.71 (p, 2H), 2.88 (t, 2H).

2.14 General Procedure for the Formation of C_{16}–C_{22} Acid Chlorides

A solution of the appropriate acid (12.0 mmol) and thionyl chloride (35 mL) was allowed to stir for 2 h at 50 ºC. The reaction mixture was concentrated, then a chase solvent was added and the mixture re-concentrated. This was performed four times, first with toluene (2 × 30 mL) and then dichloromethane (2 × 30 mL). The light brown oil was dried under high vacuum for 24 h (96–99%). The light brown oil or white solid was used in the next step without further purification.

2.15 Experimental Procedure for the Formation of C_{16}–C_{22} Acid Chlorides

Experimental Procedure for the Formation of Hexadecanoyl Chloride

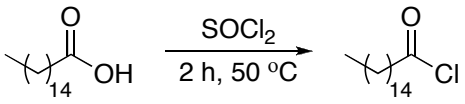

The general procedure described in Section 2.14 afforded a light brown oil (3.4921 g, 12.7 mmol, 99%): ^{1}H NMR ($CDCl_3$) δ 0.88 (t, 3H), 1.26 (m, 24H), 1.71 (p, 2H), 2.88 (t, 2H).

Experimental Procedure for the Formation of Octadecanoyl Chloride

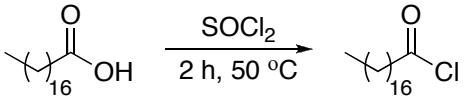

The general procedure described in Section 2.14 afforded a white solid (10.2772 g, 33.9 mmol, 96%): ^{1}H NMR ($CDCl_3$) δ 0.88 (t, 3H), 1.26 (m, 28H), 1.71 (p, 2H), 2.88 (t, 2H).

Experimental Procedure for the Formation of Icosanoyl Chloride

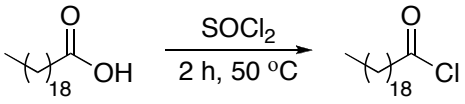

The general procedure described in Section 2.14 afforded a white solid (3.6904 g, 11.2 mmol, 99%): ^{1}H NMR ($CDCl_3$) δ 0.88 (t, 3H), 1.26 (m, 32H), 1.71 (p, 2H), 2.88 (t, 2H).

Experimental Procedure for the Formation of Docosanoyl Chloride

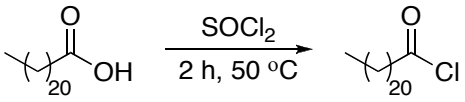

The general procedure described in Section 2.14 afforded a white solid (3.8150 g, 10.6 mmol, 99.%): ^{1}H NMR ($CDCl_3$) δ 0.88 (t, 3H), 1.26 (m, 36H), 1.71 (p, 2H), 2.88 (t, 2H).

2.16 Experimental Procedure for the Formation of Di-*tert*-butyl 4-Methyl-4-(1-oxooctadecylamino)heptanedioate, 2EAm17

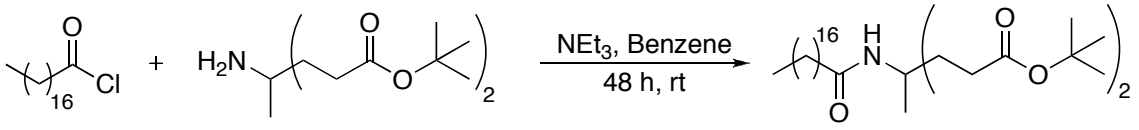

Diesteramine **2** (6.0788 g, 20.2 mmol) was dissolved in dry benzene (55 mL). Triethylamine (2.2 mL, 16 mmol) and octadecanoyl chloride (4.1501 g, 13.7 mmol) were added to the stirring diesteramine solution. The addition resulted immediately in a cloudy solution. The solution was stirred for 48 h at rt. The reaction mixture was washed with saturated $NaHCO_3$ (1 × 55 mL), water (1 × 55 mL), 10% aq HCl (1 × 55 mL), and saturated NaCl (1 × 55 mL). The solution was dried with $MgSO_4$. After filtration the solution was concentrated and the light brown solid was recrystallized three

times from acetonitrile to produce a white solid (2.6872 g, 4.73 mmol, 34.5%): mp 57.1–57.8 °C; ^{1}H NMR ($CDCl_3$) δ 0.88 (t, 3H), 1.25 (m, 31H), 1.44 (s, 18H), 1.58 (bm, 2H), 1.88 (dt, 2H), 2.06 (m, 4H), 2.24 (t, 4H), 5.69 (s, 1H); ^{13}C NMR ($CDCl_3$) δ 14.3, 22.8, 23.9, 26.0, 28.2, 29.45, 29.50, 29.53, 29.7, 29.81, 29.85, 30.5, 32.1, 33.5, 37.8, 55.3, 80.7, 172.9, 173.4; IR 3332, 2917, 2849, 1723, 1645, 1542, 1151 cm^{-1}; HRMS (FAB+) calcd for $C_{34}H_{66}O_5N$ $[M+H]^+$ 568.4943, found 568.4949; Anal. Calcd for $C_{34}H_{65}O_5N$ C, 71.91; H, 11.54; N, 2.47. Found C, 72.05; H, 11.54; N, 2.45.

2.17 General Procedure for the Formation of 2EAm13, 15, 19, 21

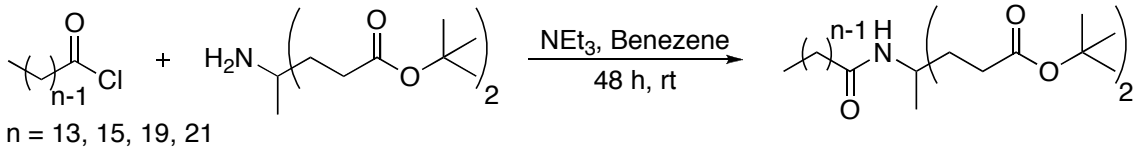

n = 13, 15, 19, 21

Diesteramine **2** (8.0 mmol) was dissolve in dry benzene (35 mL). Triethylamine (9.6 mmol) and the appropriate acid chloride (8.4 mmol) were added to the flask. The addition resulted immediately in a cloudy solution. The solution was stirred for 48 h at rt. The reaction mixture was washed with saturated $NaHCO_3$ (1 × 35 mL), water (1 × 35 mL), 10% aq HCl (1 × 35 mL), and saturated NaCl (1 × 35 mL). The light brown solution was dried with $MgSO_4$. After filtration the solution was concentrated and dried under a high vacuum for 24 h to produce a light brown oil or an off-white solid. The oil or solid was purified in two batches (~2 g each) by flash chromatography with silica gel (91 g, 15.2 × 4.4 cm column) to produce a white solid (76–78%).

2.18 Experimental Procedure for the Formation of 2EAm13, 15, 19, 21

Experimental Procedure for the Formation of Di-*tert*-butyl 4-Methyl-4-(1-oxotetradecylamino)heptanedioate, 2EAm13

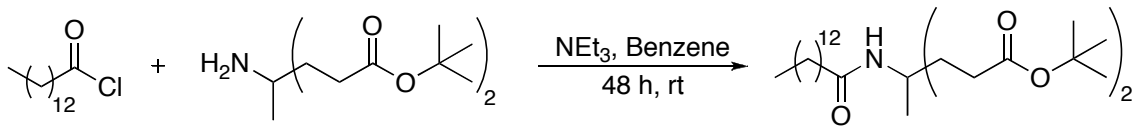

The general procedure from Section 2.17 was used to produced a clear oil, which solidified overnight to a white solid (3.4491 g, 6.74 mmol, 77%): mp 42.9–43.2 °C; ^{1}H NMR ($CDCl_3$) δ 0.88 (t, 3H), 1.25 (m, 23H), 1.44 (s, 18H), 1.58 (bt, 2H), 1.88 (m, 2H), 2.08 (m, 4H), 2.24 (t, 4H), 5.70 (s, 1H); ^{13}C NMR ($CDCl_3$) δ 14.3, 22.8, 23.9, 26.0, 28.2, 29.44, 29.49, 29.52, 29.66, 29.78, 29.80, 29.83, 30.5, 32.1, 33.5, 37.8, 55.3, 80.7, 172.9, 173.4; IR 3304, 2921, 2851, 1726, 1644, 1544, 1148 cm^{-1}; HRMS (FAB+) calcd for $C_{30}H_{58}O_5N$ $[M+H]^+$ 512.4318, found ; Anal. Calcd for $C_{30}H_{57}O_5N$ C, 70.41; H, 11.23; N, 2.74. Found C, 70.33; H, 11.31; N, 2.66.

Experimental Procedure for the Formation of Di-*tert*-butyl 4-Methyl-4-(1-oxohexadecylamino)heptanedioate, 2EAm15

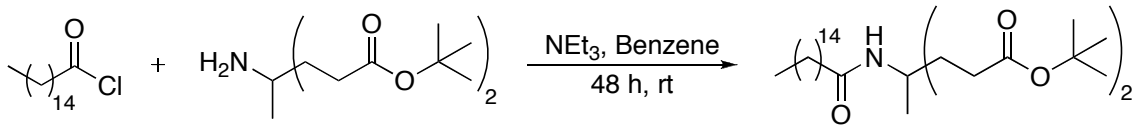

The general procedure from Section 2.17 was used to produced a white solid (3.5419 g, 6.56 mmol, 77%): mp 46.2– 46.6°C; ^{1}H NMR ($CDCl_3$) δ 0.88 (t, 3H), 1.25 (m, 27H), 1.44 (s, 18H), 1.58 (bq, 2H), 1.88 (m, 2H), 2.06 (m, 4H), 2.24 (t, 4H), 5.70 (s, 1H); ^{13}C NMR ($CDCl_3$) δ 14.1, 22.7, 23.8, 25.8, 28.0, 29.28, 29.35, 29.37, 29.5, 29.62, 29.64, 29.67, 29.68, 30.3, 31.9, 33.3, 37.6, 55.2, 80.5, 172.7, 173.2; IR 3304, 2920, 2851, 1725,

1644, 1543, 1148 cm^{-1}; HRMS (FAB+) calcd for $C_{32}H_{62}O_5N$ $[M+H]^+$ 540.4630, found 540.4644; Anal. Calcd for $C_{32}H_{61}O_5N$ C, 71.20; H, 11.39; N, 2.59. Found C, 71.37; H, 11.23; N, 2.58

Experimental Procedure for the Formation of Di-*tert*-butyl 4-Methyl-4-(1-oxoicosylamino)heptanedioate, 2EAm19

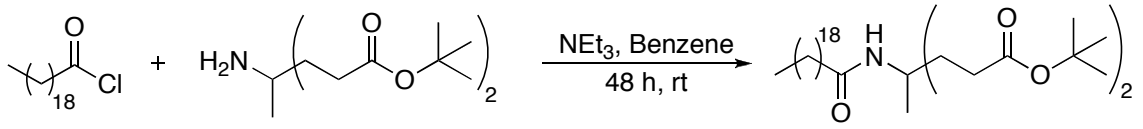

The general procedure from Section 2.17 was used to produce a white solid (3.5274 g, 5.92 mmol, 75%): mp 61.9–62.7 °C; ^{1}H NMR ($CDCl_3$) δ 0.88 (t, 3H), 1.25 (m, 35H), 1.44 (s, 18H), 1.58 (bm, 2H), 1.88 (dt, 2H), 2.08 (m, 4H), 2.24 (t, 4H), 5.70 (s, 1H); ^{13}C NMR ($CDCl_3$) δ 14.3, 22.8, 23.9, 25.9, 27.3, 28.2, 29.1, 29.4, 29.50, 29.52, 29.66, 29.79, 29.84, 30.4, 32.1, 33.5, 37.8, 55.3, 80.7, 172.9, 173.4; IR 3328, 2916, 2848, 1723, 1645, 1542, 1154 cm^{-1}; HRMS (FAB+) calcd for $C_{36}H_{70}O_5N$ $[M+H]^+$ 596.5256, found 596.5309; Anal. Calcd for $C_{36}H_{69}O_5N$ C, 72.56; H, 11.67; N, 2.35. Found C, 72.62; H, 11.72; N, 2.34.

Experimental Procedure for the Formation of Di-*tert*-butyl 4-Methyl-4-(1-oxodocosylamino)heptanedioate, 2EAm21

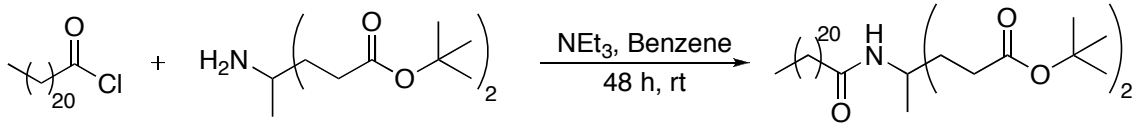

The general procedure from Section 2.17 was used to produced a white solid (3.6395 g, 5.83 mmol, 78%): mp 66.4–67.2 °C; ^{1}H NMR ($CDCl_3$) δ 0.88 (t, 3H), 1.25 (m, 39H), 1.44 (s, 18H), 1.58 (bm, 2H), 1.88 (dt, 2H), 2.08 (m, 4H), 2.24 (t, 4H), 5.70 (s,

1H); ^{13}C NMR ($CDCl_3$) δ 14.3, 22.8, 23.9, 25.9, 27.3, 28.2, 29.1, 29.44, 29.50, 29.52, 29.66, 29.79, 29.84, 30.4, 32.1, 37.8, 55.3, 80.7, 172.9, 173.4; IR 3335, 2918, 2849, 1724, 1646, 1543, 1155 cm^{-1}; HRMS (FAB+) calcd for $C_{38}H_{74}O_5N$ $[M+H]^+$ 624.5569, found ; Anal. Calcd for $C_{38}H_{73}O_5N$ C, 73.14; H, 11.79; N, 2.24. Found C, 73.00; H, 11.79; N, 2.21.

2.19 Experimental Procedure for the Formation of 4-Methyl-4-(1-oxooctadecylamino)heptanedioic Acid, 2CAm17

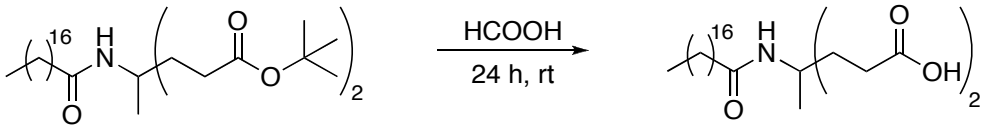

Formic acid (20 mL) and unstabilized THF (2.25 mL) were added to **2EAm17** (2.2363 g, 3.94 mmol) resulting in a slightly cloudy solution. The reaction mixture was stirred for 24 h at rt resulting in a thick white solution. The mixture was concentrated, then a chase solvent was added and the mixture was re-concentrated. This was performed with dichloromethane (2 × 30 mL) to produce a white solid, which was recrystallized twice from glacial acetic acid. Acetone (35 mL) was added to the white solid as a chase solvent and concentrated. This was repeated once more with acetone (35 mL) and dichloromethane (2 × 35 mL). The white solid was dried under high vacuum for 48 h (1.4213 g, 3.12 mmol, 79%): mp 133.6–134.0 °C; ^{1}H NMR (CD_3OD) δ 0.89 (t, 3H), 1.21 (s, 3H), 1.28 (m, 28H), 1.58 (bq, 2H), 1.84 (m, 2H), 2.14 (t, 2H), 2.26 (m, 6H), 7.41 (s, 1H); ^{13}C NMR (DMSO-d_6) δ 14.0, 22.1, 23.3, 25.5, 28.64, 28.66, 28.74, 28.82, 29.00. 29.04, 29.07, 31.3, 32.8, 35.9, 54.0, 172.0, 174.7; IR 3404, 2916, 2848, 1723, 1689, 1614, 1521 cm^{-1}; HRMS (FAB+) calcd for $C_{26}H_{50}O_5N$ $[M+H]^+$ 456.3690, found

456.3694; Anal. Calcd for $C_{26}H_{49}O_5N$ C, 68.53; H, 10.84; N, 3.07. Found C, 68.70; H, 10.86; N, 3.06.

2.20 General Procedure for the Formation of 2CAm13, 15, 19, 21

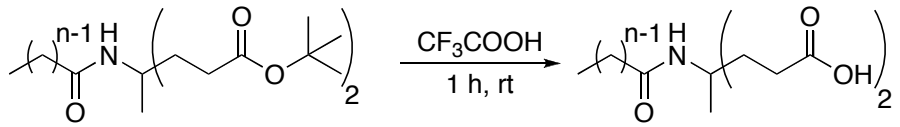

n = 12, 14 18, 20

Trifluoroacetic acid (3.5 mL) was added to the appropriate long-chain ester (5 mmol) and stirred for 1 h at rt. The light yellow solution was concentrated, then a chase solvent was added and the mixture was re-concentrated. This was performed with dichloromethane (10 mL) repeatedly until an off-white solid appeared. The off-white solid was recrystallized either from glacial acetic acid of 95% ethanol to produce a white solid (39–57%). The white solid was dried under high vacuum for 48 h.

2.21 Experimental Procedure for the Formation of 2CAm13, 15, 19, 21

Experimental Procedure for the Formation of 4-Methyl-4-(1-oxotetradecylamino)heptanedioic Acid, 2CAm13

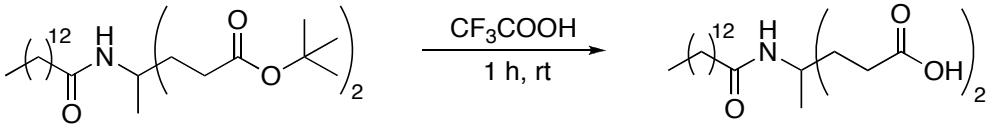

The general procedure from Section 2.20 was used to produce an off-white solid, which was recristallized twice from glacial acetic acid to yield a white solid (1.2280 g, 3.07 mmol, 53%): mp 127.5–128.2 °C; ^{1}H NMR (CD_3OD) δ 0.90 (t, 3H), 1.22 (s, 3H), 1.29 (m, 20H), 1.58 (bq, 2H), 1.85 (m, 2H), 2.15 (t, 2H), 2.27 (m, 6H); ^{13}C NMR (DMSO-d_6) δ 14.0, 22.1, 23.3, 25.5, 28.61, 28.65, 28.71, 28.78, 28.97, 29.02, 29.04, 29.06, 31.3, 32.8, 54.0, 172.0, 174.7; IR 3407, 2915, 2848, 1725, 1687, 1618, 1521 cm^{-1};

HRMS (FAB+) calcd for $C_{22}H_{42}O_5N$ $[M+H]^+$ 400.3064, found 400.3072; Anal. Calcd for $C_{22}H_{41}O_5N$ C, 66.13; H, 10.34; N, 3.51. Found C, 66.35; H, 10.45; N, 3.47.

Experimental Procedure for the Formation of 4-Methyl-4-(1-oxohexadecylamino)heptanedioic Acid, 2CAm15

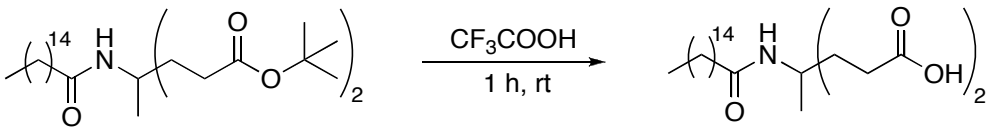

The general procedure from Section 2.20 was used to produce an off-white solid, which was recristallized three times from glacial acetic acid to yield a white solid (.9501 g, 2.22 mmol, 39%): mp 131.3–131.8 °C; ^{1}H NMR (CD_3OD) δ 0.90 (t, 3H), 1.21 (s, 3H), 1.29 (m, 24H), 1.58 (bq, 2H), 1.85 (m, 2H), 2.15 (t, 2H), 2.27 (m, 6H); ^{13}C NMR (DMSO-d_6) δ 14.0, 22.2, 23.3, 25.47, 25.51, 28.67, 28.78, 28.86, 29.04, 29.08, 29.11, 29.12, 31.4, 32.81, 32.85, 35.9, 54.0, 172.1, 174.7; IR 3364, 2916, 2848, 1725, 1689, 1618, 1519 cm^{-1}; HRMS (FAB+) calcd for $C_{24}H_{46}O_5N$ $[M+H]^+$ 428.3377, found 428.3358; Anal. Calcd for $C_{24}H_{45}O_5N$ C, 67.41; H, 10.41; N, 3.28. Found C, 67.44; H, 10.72; N, 3.27.

Experimental Procedure for the Formation of 4-Methyl-4-(1-oxoicosylamino)heptanedioic Acid, 2CAm19

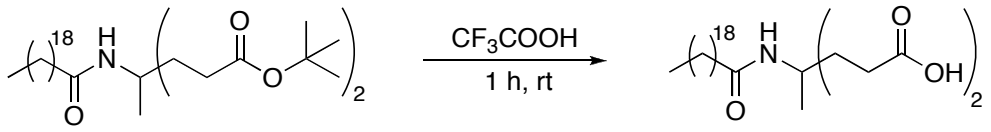

The general procedure from Section 2.20 was used to produce an off-white solid, which was recristallized three times from 95% ethanol to yield a white solid (1.3827 g, 2.86 mmol, 57%): mp 133.7–134.6 °C; ^{1}H NMR (CD_3OD) δ 0.90 (t, 3H), 1.22 (s, 3H), 1.29 (m, 32H), 1.58 (bq, 2H), 1.85 (m, 2H), 2.15 (t, 2H), 2.27 (m, 6H); ^{13}C NMR

(DMSO-d_6) δ 14.0, 22.1, 23.3, 25.5, 28.64, 28.65, 28.74, 28.83, 29.01, 29.03, 29.06, 31.3, 32.8, 35.9, 54.0, 172.0, 174.7; IR 3386, 2915, 2848, 1722, 1692, 1613, 1537 cm^{-1}; HRMS (FAB+) calcd for $C_{28}H_{54}O_5N$ $[M+H]^+$ 484.4003, found 484.3981; Anal. Calcd for $C_{28}H_{53}O_5N$ C, 69.52; H, 11.04; N, 2.90. Found C, 69.79; H, 11.13; N, 2.90.

Experimental Procedure for the Formation of 4-Methyl-4-(1-oxodocosylamino)heptanedioic Acid, 2CAm21

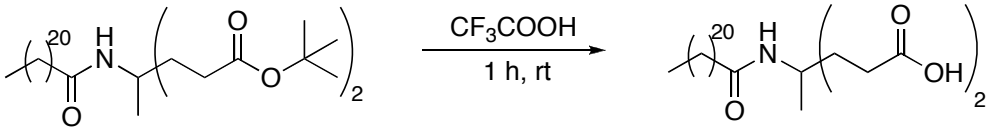

The general procedure from Section 2.20 was used to produce an off-white solid, which was recrystallized four times from glacial acetic acid to yield an impure solid. This solid was recrystallized three times from 95% ethanol to yield a white solid (.9770 g, 1.91 mmol, 39%): mp 134.5–135.4 °C; ^{1}H NMR (CD_3OD) δ 0.90 (t, 3H), 1.22 (s, 3H), 1.29 (m, 36H), 1.58 (bq, 2H), 1.86 (m, 2H), 2.15 (t, 2H), 2.27 (m, 6H); ^{13}C NMR (DMSO-d_6) δ 14.0, 22.1, 23.3, 28.64, 28.65, 28.73, 28.83, 29.01, 29.03, 29.04, 29.06, 31.3, 32.8, 54.0, 172.0, 174.7; IR 3385, 2916, 2849, 1723, 1693, 1614, 1537 cm^{-1}; HRMS (FAB+) calcd for $C_{30}H_{58}O_5N$ $[M+H]^+$ 512.4316, found 512.4301; Anal. Calcd for $C_{30}H_{57}O_5N$ C, 70.41; H, 11.23; N, 2.74. Found C, 70.59; H, 11.31; N, 2.72.

2.22 References for Chapter 2

1. Newkome, G.R., He, E., Godinez, L. A., Baker, G. R., *Electroactive metallomacromolecules via tetrabis(2,2':6',2"-terpyridine)ruthenium(II) complex: dendritic nanonetworks towards constitutional isomers and neutral species without external counterions.* J. Am. Chem. Soc., 2000. 122: p. 9993-10006.
2. Newkome, G.R., Kim, H. J., Moorfield, C. N., Maddi, H., Yoo, K., *Synthesis of new 1 → (2 + 1) C-branched monomers for the construction of multifunctional dendrimers.* Macromolecules, 2003. 36: p. 4345-4354.

3. Tishkov, A.A., Smirnov, V. O., Nefed'eva, M. V., Lyapkalo, I. M., Semenov, S. E., Ioffe, S. L., Strelenko, Y. A., Tartakovskii, V. A., *General synthesis of ϒ-functionalized β-aryl-substituted primary nitro compounds.* Russ. J. Org. Chem., 2001. 37(3): p. 390-394.
4. Newkome, G.R., Behera, R. K., Moorfield, C. N., Baker G. R., *Cascade polymers: syntheses and characterization of one-directional arbonols based on adamantane.* J. Org. Chem, 1991. 56(25): p. 7162-7167.
5. Akpo, C., Weber, E., Reiche, U., *synthesis, langmuir and langmuir-blodgett film behavior if new dendritic amphiphiles.* New J. Chem, 2006. 30(12): p. 1820-1833.
6. Holden, D.A., Ringsdorf, H., Haubs, M., *Photosensitive monolayers. photochemistry of long-chain diazo and azide compounds at the air-water interface.* J. Am. Chem. Soc, 1984. 106(16): p. 4531-4536.
7. Williams, A.A., Sugandhi, E. W., Macri, R. V., Falkinham, J. O. III, Gandour, R. D., *Antimicrobial activity of long-chain, water-soluble, dendritic tricarboxylato amphiphiles.* J. Antimicrob. Chemother., 2007. 59: p. 451-458.
8. Williams, A.A., Day, B. S., Kite, B. L., McPherson, M. K., Slebodnick, C., Morris, J. R., Gandour, R. D., *Homologous, long-chain alkyl dendrons from homologous thin films on silver oxide surfaces*. Chem. Commun., 2005(40): p. 5053-5055.
9. Adamczyk, M., Chen, Y., Johnson, D., Mattingly, P. G., Moore, J. A., Pan, Y., Reddy, R. E., *Chemiluminescent acridinium-9-carboxamide boronic acid probes: Application to a homogeneous glycated hemoglobin assay.* Bioorg. Med. Chem. Lett., 2006. 16(5): p. 1324-1328.
10. Kleinert, M., Röckendorf, N., Lindhorst, T. K., *Glyco-SAMs as glycocalyx mimetics: synthesis of L-fucose- and D-mannose- terminated building blocks.* Eur. J. Org. Chem., 2004: p. 3931-3940.
11. Röckendorf, N., Lindhorst, T. K., *Glucuronic acid derivatives as branching units for the synthesis of glycopeptide mimetics.* J. Org. Chem, 2004. 69: p. 4441-4445.
12. Newkome, G.R., Childs, B. J., Rourk, M. J., Baker, G. R., Moorefield, C. N., *Dendrimer construction and macromolecular property modification via combinatorial methods.* Biotechnol. Bioeng, 1999. 61(4): p. 243-253.
13. Newkome, G.R., *Heterocyclic loci within cascade dendritic macromolecules.* J. Heterocycl. Chem., 1996. 33(5): p. 1445-1460.
14. Newkome, G.R., Godinez, L. A., Moorefield, C. N., *Molecular recognition using beta-cyclodextrin-modified dendrimers: novel building blocks for convergent self-assembly.* Chem. Commun., 1998. 17: p. 1821-1822.

Chapter 3: Critical Micelle Concentrations for the 2CAmn Series

3.1 Introduction to CMC

In order to understand the mechanism of antimicrobial activity of these amphiphiles, we must measure the CMC for each series of amphiphile. The CMC is the concentration at which micelles spontaneously form. This value is important to measure because micelle formation is associated with detergency[1], a possible mechanism for antimicrobial activity. As stated in Chapter 1, we want to make amphiphiles that have low MICs and high CMCs to reduce the likelihood of detergency being a mechanism of action.

3.2 CMC Results

CMC data were collected with a pendent-drop analyzer to measure surface tension. Surface tension and gravity determines the shape of a drop[2]. High surface tension (little to no amphiphile present, Figure 3.1a) will give a drop with a more spherical shape compared to a drop that has low surface tension (higher concentration of amphiphile, Figure 3.1b). A camera records the shape of a drop hanging at the tip of a needle and uses the Laplace-Young equation (Equation 3.1) to determine the surface tension[3]. Where ΔP is the pressure difference across the liquid-air interface, and γ is the surface tension. R_1 and R_2 are the two principal radii of curvature, where R_1 and R_2 are equal if the drop is spherical. $\Delta\rho$ is the density difference between the liquid-air interface, g is the acceleration of gravity and h is the height of the drop.

$$\Delta P = \gamma\left(\frac{1}{R_1}+\frac{1}{R_2}\right)=\Delta\rho gh \qquad \text{Equation 3.1}$$

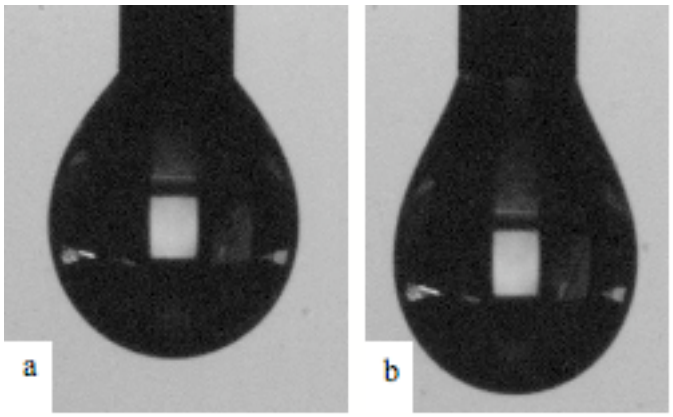

Figure 3.1 Drop shape at high and low surface tension. a. 15 μL of water. b. 15 μL of a 3000 mg/L solution of **2CAm13**.

A series of dilutions were prepared for each of the **2CAmn** amphiphiles in an aqueous triethanolamine (TEA) solution, and then the surface tension for a drop was measured. Surface tension decreases with increasing concentration of amphiphile up to the CMC, where the surface tension levels off with increasing concentrations of amphiphile[4].

Plots of interfacial tension (IFT) versus log[amphiphile] were prepared for each amphiphile. Figure 3.2 shows decreasing surface tension with increasing concentration of **2CAm21** to the CMC (dashed line), where the surface tension levels off. The CMC for **2CAm21** is 85 mg/L or 170 μM.

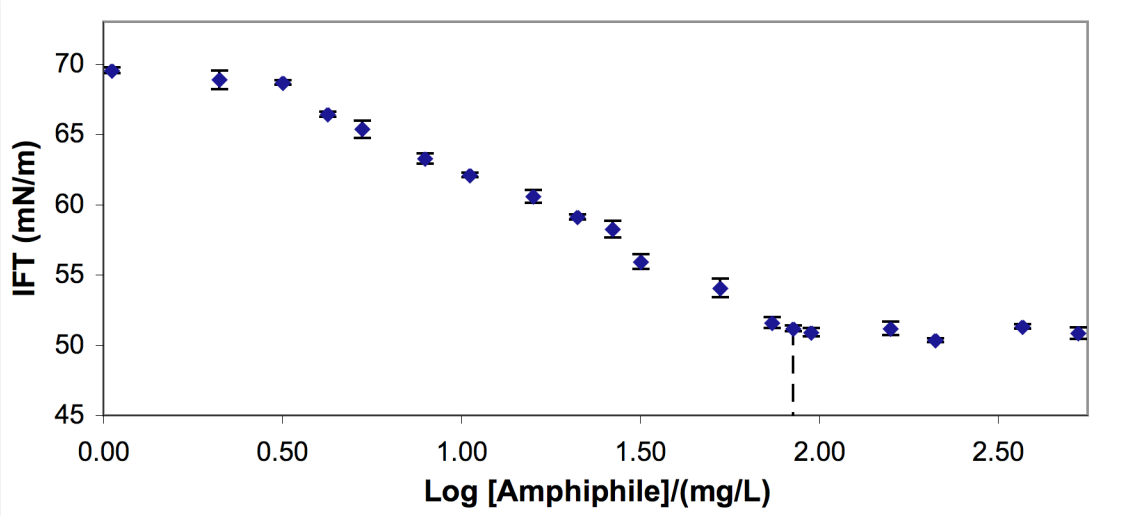

Figure 3.2 IFT vs. log of amphiphile concentration for **2CAm21**

The surface tension plot for **2CAm19** (Figure 3.3) shows a similar trend to **2CAm21**. The CMC was determined to be 360 mg/L or 740 µM (dashed line on Figure 3.3).

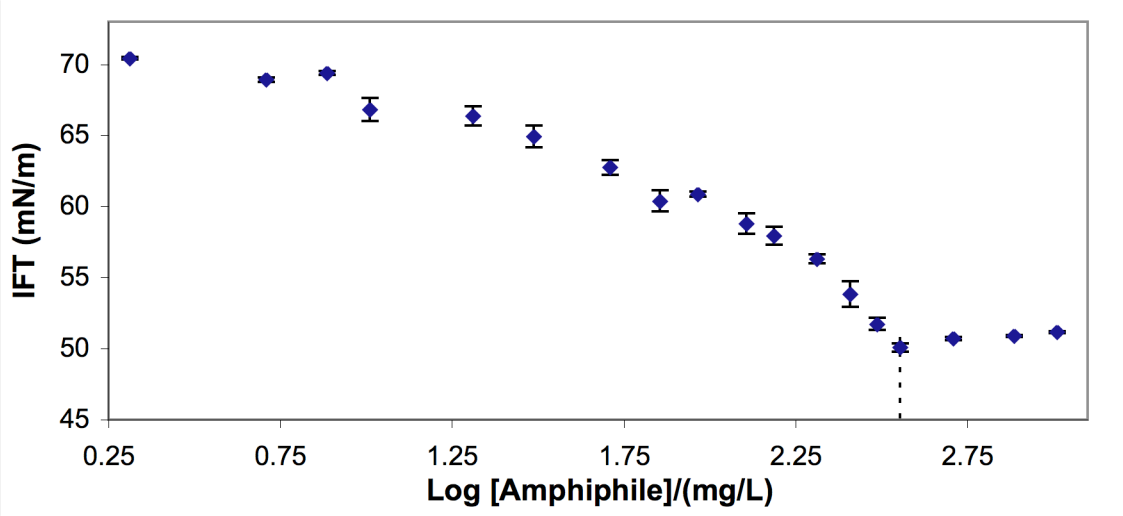

Figure 3.3 IFT vs. log of amphiphile concentration for **2CAm19**

The surface tension plot for **2CAm17** (Figure 3.4) shows a similar trend to both **2CAm19** and **2CAm21**. The CMC was determined to be 1000 mg/L or 2200 µM (dashed line on Figure 3.4).

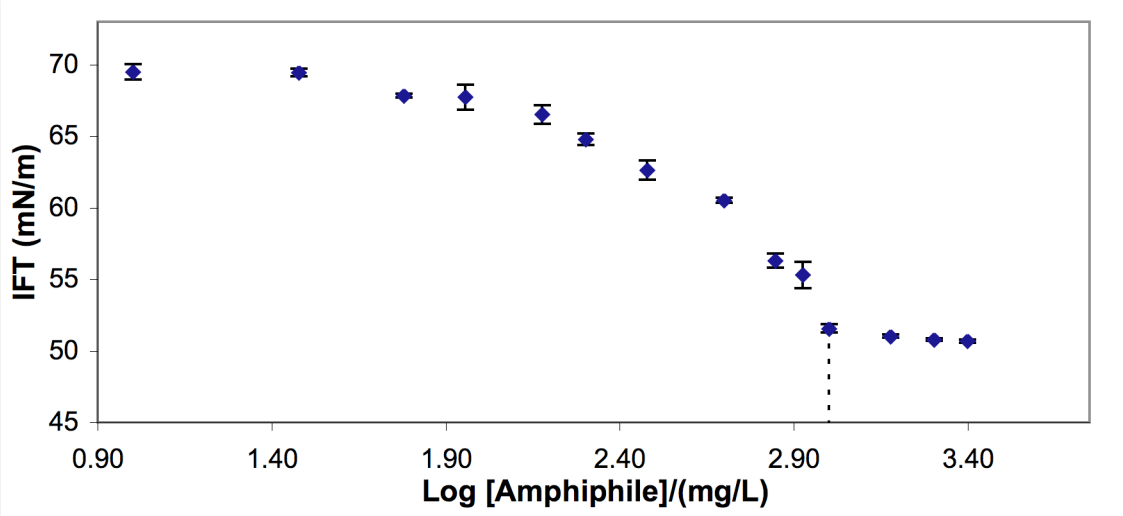

Figure 3.4 IFT vs. log of amphiphile concentration for **2CAm17**

The surface tension plot for **2CAm15** (Figure 3.5) shows a different trend from the three previous amphiphiles (Figures 3.2–3.4). The surface tension reaches a minimum at about 50 mN/m, after which the surface tension raises and levels off at higher concentrations of amphiphile. The CMC was determined to be 4100 mg/L or 9600 μM (dashed line on Figure 3.5, see Section 3.3).

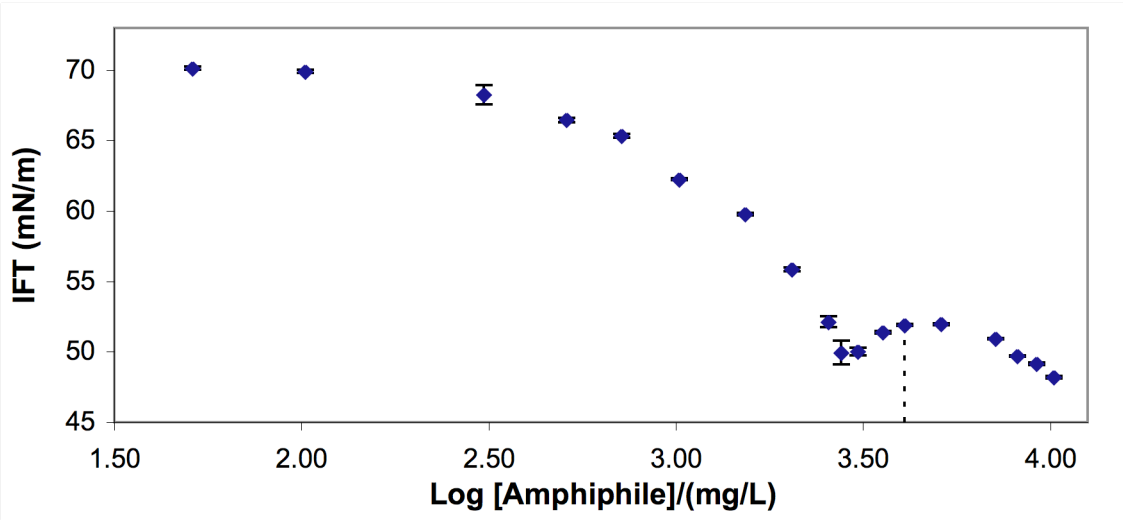

Figure 3.5 IFT vs. log of amphiphile concentration for **2CAm15**

The surface tension plot for **2CAm13** (Figure 3.6) shows a similar trend to **2CAm15** (Figure 3.5). The surface tension reaches a minimum at about 35 mN/m, after

which the surface tension raises and levels off at higher concentrations of amphiphile. The CMC was determined to be at 12000 mg/L or 30000 μM (dashed line on Figure 3.6, see Section 3.3).

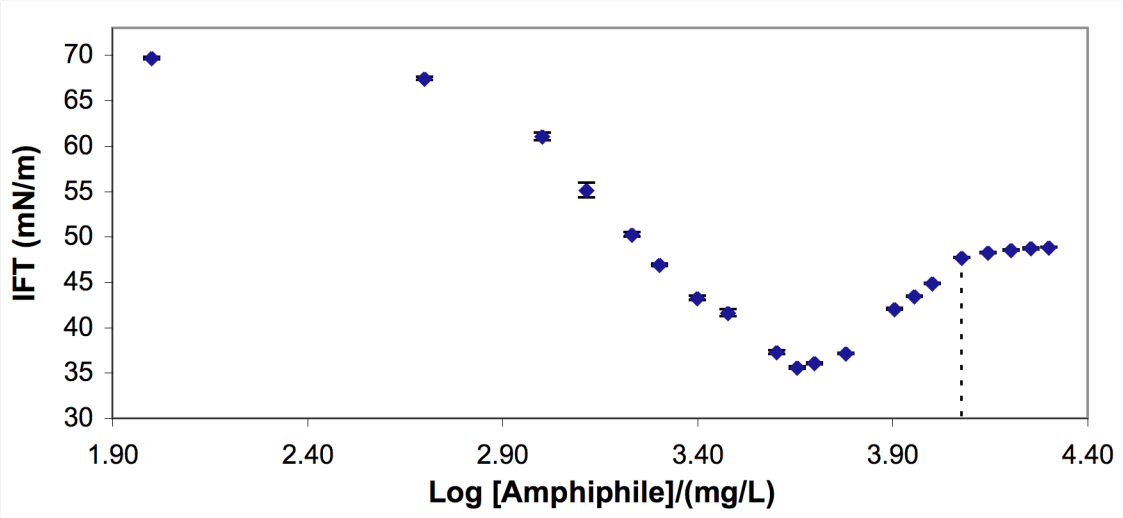

Figure 3.6 IFT vs. log of amphiphile concentration for **2CAm13**

3.3 Impurities in CMC Measurements

During the measurements of the **2CAmn** series, we noted that the surface tension plots for **2CAm15** (Figure 3.5) and **2CAm13** (Figure 3.6) were different from the rest (Figures 3.2–3.4). For **2CAm15** and **2CAm13** the surface tension has a minimum, after which the surface tension increases and levels off with increasing concentration of amphiphile. From work reported by Lin et al.,[5] this minimum is likely caused by an impurity in the sample. The CMC value in these cases is the point at which the surface tension increases and levels off (dashed lines on Figures 3.5 and 3.6).

Work performed by Lin et al.[5] studies the surface tension of a series of sodium dodecyl sulfate (SDS) solutions. Laboratory-grade SDS shows a minimum in plots of surface tension versus log concentration, which is caused by the highly surface-active lauryl alcohol impurity. The more surface-surface active lauryl alcohol lowers the

surface tension below that of SDS. When micelles begin to form, the impurity becomes solubilized in the micelle and increases the surface tension. Conductivity measurements, which are insensitive to impurities, were performed on the SDS samples to compare the CMC value from both methods. The CMC values from the conductivity measurements matched the point when the surface tension increases and levels off.

The measurement of surface tension can be a test for surfactant impurities. As little as 0.01% of an impurity can cause the surface tension to decrease and display a minimum[4]. Even though all homologues of the **2CAmn** series have passed elemental analysis (see Chapter 2), there may be a very small amount of impurity that causes the minimum in surface tension for **2CAm15** (Figure 3.5) and **2CAm13** (Figure 3.6). It is possible that contamination occurred during the preparation of samples used for surface tension measurements. It is also important to note that the samples prepared for surface tension measurements contain an excess of triethanolamine (between 1.2–15000 mole excess). This excess in combination with the possible loose micelle structure of the **2CAmn** series may have an effect on surface tension (Figure 3.7). Even with impurities, the CMC values can be measured for all the amphiphiles in the **2CAmn** series (see below).

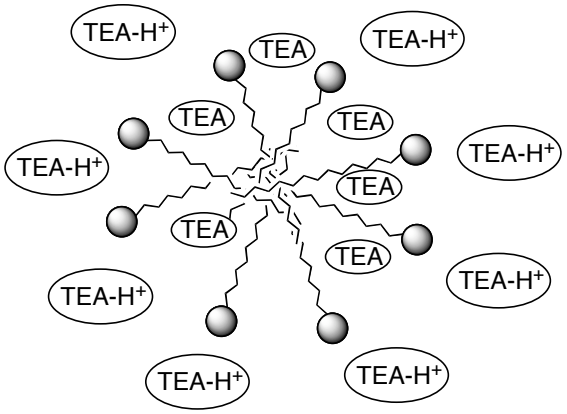

Figure 3.7 Possible effect of excess TEA on micelle structure. Where TEA is $N(CH_2CH_2OH)_3$ and TEA-H^+ is $^+NH(CH_2CH_2OH)_3$.

3.4 Discussion of CMC Results

The results for the **2CAmn** series (Figure 3.8) show a linear relationship between log CMC and chain length with a slope of –0.28 ± 0.01. Although the **2CAm15** and **2CAm13** amphiphiles contain impurities which affect the surface tension plots (Figures 3.5 and 3.6, respectivaly), the R^2 value for the **2CAmn** series (Figure 3.8) is 0.99. The significance of this observation is that CMC values can be measured, even with impurities, to get a good linear fit within a series of amphiphiles. The **3CAmn** series also has a linear relationship with a slope of –0.17 ± 0.01. The CMCs of the triethanolammonium salts of natural, saturated fatty acids show a biphasic dependence on chain length[6]. The slopes have values of –0.031 ± 0.02 for octanoate to dodecanoate and –0.31 ± 0.09 for tetradecanoate to octadecanoate[6].

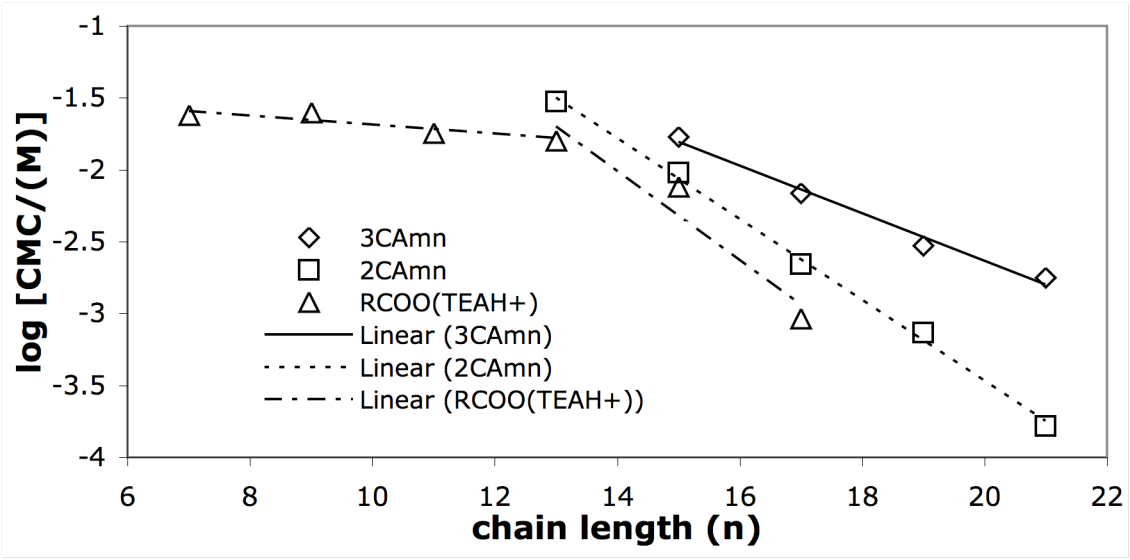

Figure 3.8 CMC Comparison

Our hypothesis (see Chapter 1, Section 1.4) for the **2CAmn** series was that the CMCs would fall in between those for the **3CAmn** and fatty acid series. From Figure 3.8 we can see that this hypothesis matches the experimental results. The two carboxyl groups in the **2CAmn** series makes the amphiphiles more soluble in aqueous media than fatty acids, but not as soluble as the **3CAmn** series with three carboxyl groups. The headgroup repulsion in the micelle is greater for the **2CAmn** series when compared to fatty acids, but less repulsive than the three carboxyl groups in the **3CAmn** series.

Comparing the log CMC versus chain length for the **2CAmn** series and the amphiphiles reported by Shinoda[7] and Paleos[8] (Figures 3.9 and 3.10, respectively) shows a similar trend to Figure 3.8. The potassium salts of fatty acids have a lower CMC value when compared to the multi-headed amphiphiles. The CMCs for the potassium salts of fatty acids[7, 8] differs from the triethanolammonium salts[6] (Figure 3.8) in that it does not show a biphasic relationship. The **2CAmn** series and the multi-headed series from Shinoda[7] and Paleos[8] have CMCs similar to one another.

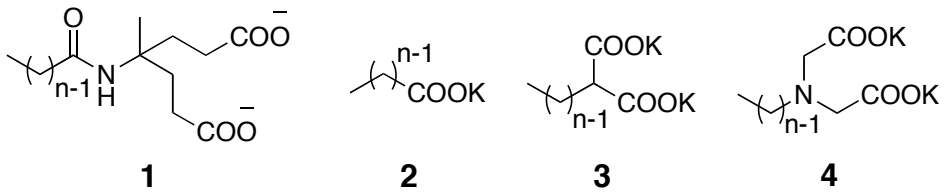

1 **2** **3** **4**

Figure 3.9 Amphiphiles compared in Figure 3.10

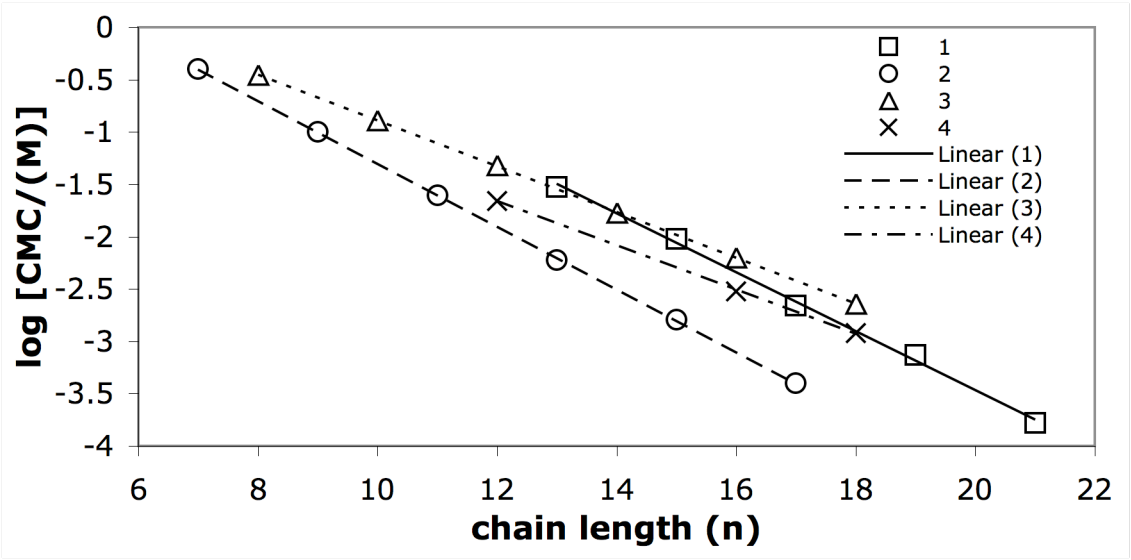

Figure 3.10 CMC Comparison for the **2CAmn** series, amphiphiles reported by Shinoda, and Paleos.

The longest two-headed amphiphiles studied by Shinoda[7] and Paleos[8] contained 18 carbons in the fatty chain. CMC measurements of longer versions of **3** and **4** (Figure 3.9) may be hard to measure due to a higher Krafft temperature. The point at which solubility equals the CMC is called the Krafft temperature (T_{Kr}). Just above this temperature, solubility increases. Amphiphile solutions cooled below their T_{Kr} may precipitate as a hydrated crystal. The packing of the crystal hydrate will depend on the structure of the amphiphile and will determine the T_{Kr}. Amphiphiles **3** and **4** (Figure 3.9) have a more rigid headgroup compared to the **2CAmn** headgroup. The less rigid **2CAmn** amphiphiles may make it hard to form a crystalline structure and may lower the T_{Kr} compared to **3** and **4** (Figure 3.9).

3.5 CMC General Methods

A video system (mounted on a vibration isolation table), which measures the surface tension of a pendent drop from an 18-gauge stainless-steel needle (1.27 mm), was used. To help maintain humidity levels and ensure that the drop size did not vary significantly during the measurements, the pendent drop was enclosed in a standard glass cuvette that contained 0.5 mL of aqueous triethanolamine (~9 mg/mL) dissolved in ultrapure (Type I) water. A hole (2.54 mm) was drilled in the Teflon™ lid to accommodate the needle. Calibration of the instrument entailed measuring the tip width of the needle with a micrometer and using that measurement to perform an initial calibration of the video camera's magnification. The calibration was further refined by then adjusting the magnification to produce a surface tension of 72.8 mN/m with a ~ 15 μL drop of ultrapure (Type 1) water at an ambient air temperature of 20 °C.

Surface tension measurements were carried out on each solution via drop-shape analysis, with each drop being measured 20 times (one measurement was made by the software every 0.5 seconds) to produce an average surface tension. Reproducibility of the measurements was determined by performing the drop-shape analysis on five different drops of the same solution to obtain values with standard deviations of approximately ± 0.3 mN/m. Plots of surface tension versus log [amphiphile] were made; linear least-square analyses of the points before and the points after the break were used to determine the CMC. Average percent error of all measurements was 5%.

3.5.1 CMC Determination 2CAm21

The Amphiphile **2CAm21** (52.8 mg) was combined with triethanolamine (TEA, 225.5 mg) in a 25 mL volumetric flask, diluted to the mark with ultrapure (Type I) water,

and sonicated for 1 h to produce a stock solution. This stock solution (2000 mg/L) was used to generate a series of dilutions for determining the CMC, which were prepared in the following manner. The stock solution (500 ± 2 μL), measured with an autopipettor, was placed in a 20 mL scintillation vial and diluted with an aqueous solution (1500 ± 5 μL) comprised of TEA (9.090 mg/mL) in ultra pure (Type I) water. This produced a dilution solution with an amphiphile (**2CAm21**) concentration of 500 mg/L. Similar dilutions were made to produce the amphiphile concentrations in Table 3.1. Measurements of interfacial tension (IFT) were made after allowing the drop to equilibrate for 10 minutes and the results are shown on Table 3.2. The CMC was determined to be 85 mg/L or 170 μM.

Table 3.1 2CAm21 Dilutions used for measurement of IFT

Dilutions from 2000 mg/L		
Desired solution (mg/L)	**Volume of stock used (mL ± 0.002)**	**Volume of TEA solution used (mL ± 0.005)**
500	0.500	1.500
350	0.350	1.650
200	0.500	4.500
150	0.150	1.850
Dilutions from 200 mg/L		
Desired solution (mg/L)	**Volume of stock used (mL ± 0.002)**	**Volume of TEA solution used (mL ± 0.005)**
90	0.900	1.100
80	0.800	1.200
70	0.700	1.300
50	0.500	1.500
30	0.300	1.700
25	0.250	1.750
20	0.200	1.800
15	0.150	1.850
10	0.300	5.700
Dilutions from 10 mg/L		
Desired solution (mg/L)	**Volume of stock used (mL)**	**Volume of TEA solution used (mL)**
7.5	1.500 ± 0.005	0.500 ± 0.002
5	1.000 ± 0.005	1.000 ± 0.002
4	0.800 ± 0.002	1.200 ± 0.005
3	0.600 ± 0.002	1.400 ± 0.005
2	0.400 ± 0.002	1.600 ± 0.005
1	0.200 ± 0.002	1.800 ± 0.005

Table 3.2 CMC Data for **2CAm21**

Sample label	Amphiphile concentration (mg/L)	Mean IFT (mN/m)	SD
Water	0	72.7	0.1
Water/$N(EtOH)_3$	0	71.8	0.1
500	530	50.8	0.4
350	370	51.3	0.2
200	210	50.3	0.1
150	160	51.2	0.5
90	95	50.9	0.3
80	84	51.2	0.2
70	74	51.6	0.4
50	53	54.1	0.7
30	32	55.9	0.5
25	26	58.2	0.6
20	21	59.1	0.2
15	16	60.6	0.5
10	11	62.1	0.2
7.5	7.9	63.3	0.4
5	5.3	65.4	0.6
4	4.2	66.4	0.2
3	3.2	68.7	0.2
2	2.1	68.9	0.7
1	1.1	69.5	0.2

3.5.2 CMC Determination 2CAm19

The amphiphile **2CAm19** (102.3 mg) was combined with TEA (260.1 mg) is a 25 mL volumetric flask and filled to the mark with ultrapure (Type I) water to produce a stock solution (4000 mg/L), which was made in a manner analogous to that of **2CAm21**. The stock solution was diluted with an aqueous solution comprised of TEA (9.097 mg/mL) in ultrapure (Type I) water to give the amphiphile (**2CAm19**) concentration as shown in Table 3.3. Measurements of IFT were made after letting each drop equilibrate for 12 minutes and the results are shown on Table 3.4. The CMC was determined to be 360 mg/L or 740 μM.

Table 3.3 2CAm19 Dilutions used for measurement of IFT

Dilutions from 4000 mg/L		
Desired solution (mg/L)	**Volume of stock used (mL ± 0.002)**	**Volume of TEA solution used (mL± 0.005)**
1000	0.500	1.500
750	0.375	1.625
500	0.250	1.750
350	0.175	1.825
300	0.150	1.850
250	0.125	1.875
200	0.500	9.500
Dilutions from 200 mg/L		
Desired solution (mg/L)	**Volume of stock used (mL)**	**Volume of TEA solution used (mL)**
150	1.500 ± 0.005	0.500 ± 0.002
125	1.250 ± 0.005	0.750 ± 0.002
90	0.900 ± 0.002	1.100 ± 0.005
70	0.700 ± 0.002	1.300 ± 0.005
50	0.500 ± 0.002	1.500 ± 0.005
30	0.300 ± 0.002	1.700 ± 0.005
20	0.200 ± 0.002	1.800 ± 0.005
10	0.200 ± 0.002	3.800 ± 0.005
Dilutions from 10 mg/L		
Desired solution (mg/L)	**Volume of stock used (mL)**	**Volume of TEA solution used (mL)**
7.5	1.500 ± 0.005	0.500 ± 0.002
5	1.000 ± 0.005	1.000 ± 0.005
2	0.400 ± 0.002	1.600 ± 0.005

Table 3.4 CMC Data for **2CAm19**

Sample label	Amphiphile concentration (mg/L)	Mean IFT (mN/m)	SD
Water	0	72.9	0.1
Water/$N(EtOH)_3$	0	71.4	0.1
1000	1000	51.2	0.1
750	770	50.9	0.1
500	510	50.7	0.1
350	360	50.1	0.3
300	310	51.7	0.4
250	260	53.8	0.9
200	200	56.3	0.3
150	150	57.9	0.6
125	130	58.8	0.7
90	92	60.9	0.2
70	72	60.4	0.8
50	51	62.8	0.5
30	31	64.9	0.8
20	20	66.4	0.7
10	10	66.8	0.8
7.5	7.7	69.4	0.1
5	5.1	68.9	0.2
2	2.0	70.4	0.1

3.5.3 CMC Determination 2CAm17

The amphiphile **2CAm17** (200.5 mg) was combined with TEA (230.2 mg) is a 25 mL volumetric flask and filled to the mark with ultrapure (Type I) water to produce a stock solution (8000 mg/L), which was made in a manner analogous to that of **2CAm21**. The stock solution was diluted with an aqueous solution comprised of TEA (9.097 mg/mL) in ultrapure (Type I) water to give the amphiphile (**2CAm17**) concentration as shown in Table 3.5. Measurements of IFT were made after letting each drop equilibrate for 7 minutes and the results are shown on Table 3.6. The CMC was determined to be 1000 mg/L or 2200 μM.

Table 3.5 2CAm17 Dilutions used for measurement of IFT

Dilutions from 8000 mg/L		
Desired solution (mg/L)	**Volume of stock used (mL ± 0.002)**	**Volume of TEA solution used (mL ± 0.005)**
2500	0.625	1.375
2000	0.500	1.500
1500	0.375	1.625
1000	0.250	1.750
840	0.210	1.790
700	0.175	1.825
500	0.375	5.625
Dilutions from 500 mg/L		
Desired solution (mg/L)	**Volume of stock used (mL)**	**Volume of TEA solution used (mL)**
300	1.200 ± 0.005	0.800 ± 0.002
200	0.800 ± 0.002	1.200 ± 0.005
150	0.600 ± 0.002	1.400 ± 0.005
90	0.360 ± 0.002	1.640 ± 0.005
60	0.240 ± 0.002	1.760 ± 0.005
30	0.120 ± 0.002	1.960 ± 0.005
Dilutions from 30 mg/L		
Desired solution (mg/L)	**Volume of stock used (mL ± 0.002)**	**Volume of TEA solution used (mL ± 0.005)**
10	0.670	1.330

Table 3.6 CMC Data for **2CAm17**

Sample label	Amphiphile concentration (mg/L)	Mean IFT (mN/m)	SD
Water	0	72.8	0.1
Water/$N(EtOH)_3$	0	71.1	0.4
2500	2500	50.7	0.1
2000	2000	50.8	0.1
1500	1500	51.0	0.1
1000	1000	51.6	0.3
840	840	55.3	0.9
700	700	56.3	0.5
500	500	60.5	0.2
300	300	62.6	0.7
200	200	64.8	0.4
150	150	66.5	0.6
90	90	67.7	0.9
60	60	67.8	0.1
30	30	69.5	0.3
10	10	69.5	0.5

3.5.4 CMC Determination 2CAm15

The amphiphile **2CAm15** (255.4 mg) was combined with TEA (233.7 mg) is a 25 mL volumetric flask and filled to the mark with ultrapure (Type I) water to produce a stock solution (10000 mg/L), which was made in a manner analogous to that of **2CAm21**. The stock solution was diluted with an aqueous solution comprised of TEA (9.097 mg/mL) in ultrapure (Type I) water to give the amphiphile (**2CAm15**) concentration as shown in Table 3.7. Measurements of IFT were made after letting each drop equilibrate for 8 minutes and the results are shown on Table 3.8. The CMC was determined to be 4100 mg/L or 9600 μM.

Table 3.7 2CAm15 Dilutions used for measurement of IFT

Dilutions from 10000 mg/L		
Desired solution (mg/L)	**Volume of stock used (mL)**	**Volume of TEA solution used (mL)**
9000	1.800 ± 0.005	0.200 ± 0.002
8000	1.600 ± 0.005	0.400 ± 0.002
7000	1.400 ± 0.005	0.600 ± 0.002
5000	1.000 ± 0.005	1.000 ± 0.005
4000	0.800 ± 0.002	1.200 ± 0.005
3500	0.700 ± 0.002	1.300 ± 0.005
3000	0.600 ± 0.002	1.400 ± 0.005
2700	0.540 ± 0.002	1.460 ± 0.005
2500	0.500 ± 0.002	1.500 ± 0.005
2000	0.400 ± 0.002	1.600 ± 0.005
1500	0.300 ± 0.002	1.700 ± 0.005
1000	0.200 ± 0.002	1.800 ± 0.005
700	0.140 ± 0.002	1.860 ± 0.005
500	0.200 ± 0.002	3.800 ± 0.005
Dilutions from 500 mg/L		
Desired solution (mg/L)	**Volume of stock used (mL)**	**Volume of TEA solution used (mL)**
300	1.200 ± 0.005	0.800 ± 0.002
100	0.400 ± 0.002	1.600 ± 0.005
50	0.200 ± 0.002	1.800 ± 0.005

Table 3.8 CMC Data for **2CAm15**

Sample label	Amphiphile concentration (mg/L)	Mean IFT (mN/m)	SD
Water	0	72.8	0.1
Water/$N(EtOH)_3$	0	71.4	0.1
10000	10000	48.2	0.1
9000	9200	49.2	0.1
8000	8200	49.7	0.1
7000	7200	50.9	0.1
5000	5100	52.0	0.1
4000	4100	51.9	0.1
3500	3600	51.4	0.1
3000	3100	50.0	0.3
2700	2700	49.9	0.8
2500	2500	52.1	0.4
2000	2000	55.9	0.1
1500	1500	59.8	0.1
1000	1000	62.3	0.1
700	720	65.4	0.1
500	510	66.5	0.2
300	310	68.3	0.7
100	100	69.9	0.1
50	51	70.1	0.1

3.5.5 CMC Determination 2CAm13

Two stock solutions were prepared for **2CAm13**. The amphiphile **2CAm13** (99.6 mg) was combined with TEA (100.7 mg) in a 20 mL scintillation vial and dissoled with 5 mL of ultrapure (Type I) water to produce a stock solution (20000 mg/L). The amphiphile **2CAm13** (100.2 mg) was combined with TEA (94.5 mg) in a 20 mL scintillation vial and dissolved with 10 mL of ultrapure water (Type I) to produce a stock solution (10000 mg/L). Both stock solutions were sonicated for one hour. The stock solution was diluted with an aqueous solution comprised of TEA (9.097 mg/mL) in ultrapure (Type I) water to give the amphiphile (**2CAm13**) concentration as shown in Table 3.9. Measurements of IFT were made after letting each drop equilibrate for 7

minutes and the results are shown on Table 3.10. The CMC was determined to be 12000 mg/L or 30000 μM.

Table 3.9 2CAm13 Dilutions used for measurement of IFT

Dilutions from 20000 mg/L		
Desired solution (mg/L)	**Volume of stock used (mL ± 0.002)**	**Volume of TEA solution used (mL ± 0.002)**
18000	0.900	0.100
16000	0.800	0.200
14000	0.700	0.300
12000	0.600	0.400
Dilutions from 10000 mg/L		
Desired solution (mg/L)	**Volume of stock used (mL ± 0.002)**	**Volume of TEA solution used (mL ± 0.002)**
9000	0.900	0.100
8000	0.800	0.200
6000	0.600	0.400
5000	0.500	0.500
4500	0.450	0.550
4000	0.400	0.600
3000	0.300	0.700
2500	0.250	0.750
2000	0.200	0.800
1700	0.170	0.830
1300	0.130	0.870
1000	0.200	1.800 ± 0.005
Dilutions from 1000 mg/L		
Desired solution (mg/L)	**Volume of stock used (mL ± 0.002)**	**Volume of TEA solution used (mL ± 0.002)**
500	0.500	0.500
100	0.100	0.900

Table 3.10 CMC Data for **2CAm13**

Sample label	Amphiphile concentration (mg/L)	Mean IFT (mN/m)	SD
Water	0	72.8	0.1
Water/$N(EtOH)_3$	0	70.5	0.4
20000	20000	48.8	0.1
18000	18000	48.7	0.1
16000	16000	48.5	0.1
14000	14000	48.2	0.1
12000	12000	47.7	0.1
10000	10000	44.8	0.1
9000	9000	43.4	0.1
8000	8000	42.0	0.1
6000	6000	37.1	0.1
5000	5000	36.1	0.1
4500	4500	35.6	0.2
4000	4000	37.3	0.2
3000	3000	41.6	0.4
2500	2500	43.3	0.3
2000	2000	46.9	0.2
1700	1700	50.3	0.3
1300	1300	55.1	0.8
1000	1000	61.1	0.4
500	500	67.4	0.2
100	100	69.7	0.1

3.6 References for Chapter 3

1. Dennis, E.A., *Micellization and solubilization of phospholipids by surfactants.* Adv. Colloid Interface Sci., 1986. **26**: p. 155-175.
2. Evans, D.F., Wennerström, H., *The Colloidal Domain*. 2nd ed. 1999, New York: Wiley-VCH. 63.
3. *Technical documentation FTA100, FTA 200, FTA2000, FTA4000 series*, in *Laplace-Young and Bashforth-Adams equations*, First Ten Ångstroms.
4. Evans, D.F., Wennerström, H., *The Colloidal Domain*. 2nd ed. 1999, New York: Wiley-VCH. 166.
5. Lin, S., Lin, Y., Chen, E., Hsu, C., Kwan, C., *A study of the equilibrium surface tension and the critical micelle concentration of mixed surfactant solutions.* Langmuir, 1999. **15**: p. 4370-4376.
6. Bashura, A.G., Klimenko, O. I., Nurimbetov, K. N., Gladukh, E. V., *Colloidal-micellar properties of some new surfactants.* Farmatsevt. Zh. (Kiev), 1989: p. 57-58.
7. Shinoda, K., *The critical micelle concentration in aqueous solutions of potassium alkane tricarboxylates.* J. Phys. Chem., 1956. **60**: p. 1439-1441.

8. Paleos, C.M., Michas, J., Malliaris, A., *Alkyl derivatives of iminodiacetic acid: A novel class of compounds forming thermotropic liquid crystals and aqueous micelles.* Mil. Cryst. Liq. Cryst., 1990. **186**: p. 251-260.

Chapter 4: Minimal Inhibitory Concentrations (MIC) for the 2CAmn Series

4.1 Introduction to MIC

As discussed in Chapter 1, our goal is to develop new compounds as potential treatments for infections caused by *S. aureus* and MRSA. With the global threat of more antibiotic resistant strains, it is important to continue developing new drugs to fight these bacterial infections. In-vitro measurements of MIC for the **2CAmn** series against *S. aureus* and MRSA are important initial steps to gauge the potential antimicrobial activity of these amphiphiles. From the perspective of drug design, we also want to compare the activities of the two-headed (**2CAmn**) amphiphiles to those of the three-headed series (**3CAmn**, **3CUrn**, **3CCbn**).

These MIC measurements, reported below, were made by Ms. Myra Williams and Ms. Shauntrece Hardrict in Professor Falkinham's laboratory in the Department of Biological Sciences at Virginia Tech.

4.2 Results of MIC Measurements

MICs (reported as CFU/mL, Colony Forming Units/mL) of amphiphiles dissolved in aqueous trienthanolamine were measured by broth microdilutions in a 96-well microtiter plate. Control experiments demonstrated that 4% (w/v) triethanolamine/water did not inhibit the growth of any microorganisms tested. A 2-fold dilution series of the amphiphile was prepared in a 96-well microtiter plate in a 50 µL volume of 1/10-strength BHIB+S (Brain Heart Infusion Broth + Sucrose) and the dilution series was inoculated with 50 µL of each cell suspension. The resulting inoculated dilution series were incubated at 30 °C and growth, as turbidity, scored visually and recorded on the fourth

day. Activities of the amphiphiles were measured against *S. aureus* (strain ATCC 6358) and MRSA (strain ATCC 43330).

In studies [1-3] of antimicrobial activity, the MIC is often observed to increase as the initial cell density increases. This phenomenon is referred to as the "inoculum effect". The "inoculum effect" presumably reflects the increased demand for a given drug as the number of cells and targets increases. A mathematical model[4] of the "inoculum effect" describes the independence of log MIC at low inoculum be defining log MIC_0 as the intrinsic activity, log I as the inoculum, and log I_{tr} as the inoculum at the threshold immediately before the rise of MIC, and k is a constant that describes the rate of increase in MIC. Equation 4.1 is flat at low inoculum and rises exponentially when $I > I_{tr}$, which can vary by drug. In order to fit the equation to a curve, I is set to be I_{tr} when the former is smaller in value.

$$\log \text{ MIC } = \log \text{MIC}_0 + \left(e^{k(\log I - \log I_{tr})} - 1\right) \qquad \text{Equation 4.1}$$

Inoculum density affected antibacterial activity of **2CAm21** against both *S. aureus* and MRSA (Figures 4.1 and 4.2, respectively). MIC measurements at different cell densities showed that activity decreased with higher cell densities. Antibacterial activity was measured in duplicate on two separate cultures of the same bacterium. For all four series (**2CAmn**, **3CAmn**, **3CCbn**, **3CUrn**), the MIC was relatively flat between 1.6×10^2 to 1.6×10^4 CFU/mL. This flat region defines the intrinsic activity, MIC_0. Eyeball approximations were used to fit Equation 4.1 (solid line) to the inoculum data (Figures 4.1 and 4.2).

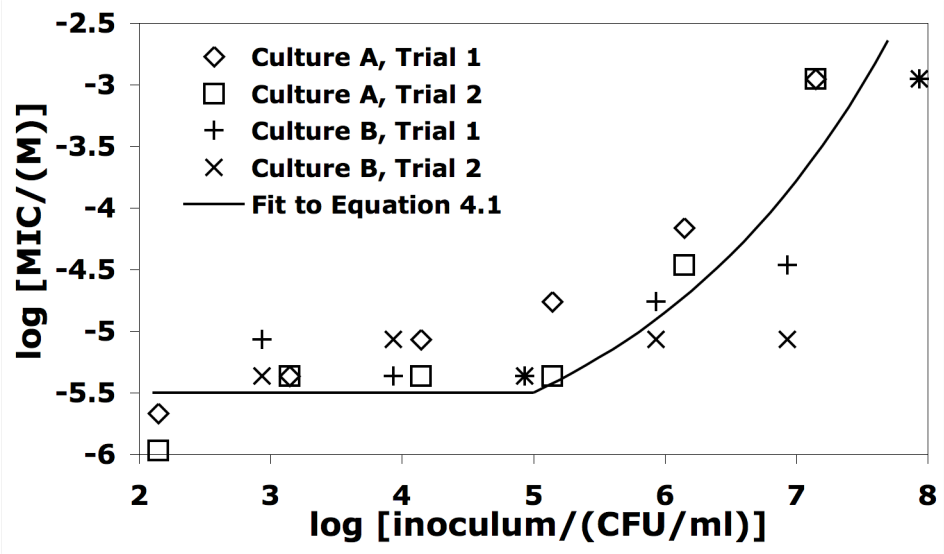

Figure 4.1 Effect of initial *S. aureus* cell density for **2CAm21**. Culture A, 1.4×10^2 to 10^7 CFU/mL; Culture B 8.6×10^2 to 10^7 CFU/mL. There is a ± 0.3 error for each measurement. For mathematical fit, log $MIC_0 = -5.5$, $k = 0.5$, log $I_{tr} = 5$, log I ranged from 2.1 – 7.9.

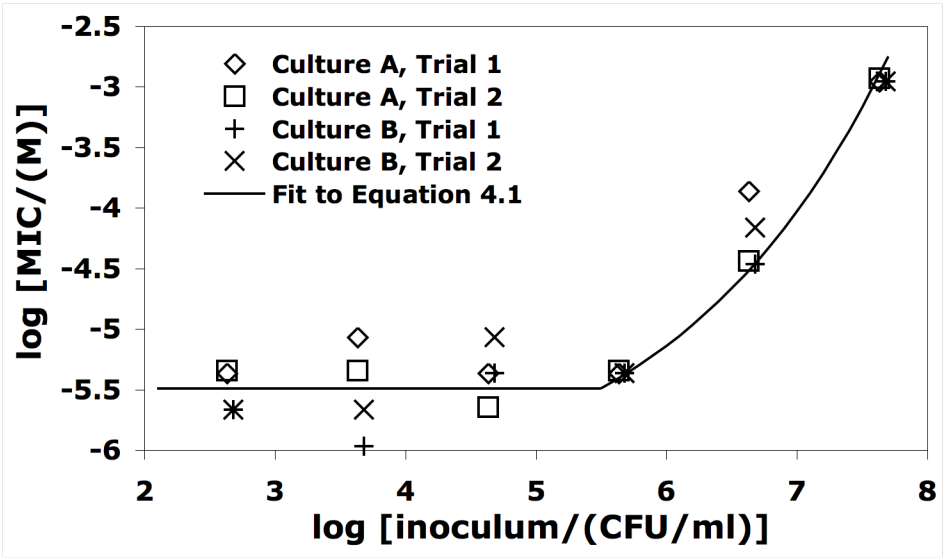

Figure 4.2 Effect of initial MRSA cell density for **2CAm21**. Culture A, 4.3×10^2 to 10^7 CFU/mL; Culture B 4.8×10^2 to 10^7 CFU/mL. There is a ± 0.3 error for each measurement. For mathematical fit, log $MIC_0 = -5.49$, $k = 0.6$, log $I_{tr} = 5.5$, log I ranged from 2.1 – 7.9.

The antibacterial activities of the **2CAmn** series against *S. aureus* and MRSA were measured at several inoculum densities. Cells were grown to the log phase. The

MICs at low densities were consistent for each homologue in the **2CAmn** series. This consistency suggests that the MICs have reached a minimum, which is defined as MIC_0[4, 5]. The values for MIC_0 for all four series were calculated by averaging all the MICs (4 to 13 measurements for *S. aureus*, 9 to 31 measurements for MRSA) for inoculum densities $\leq 3.2 \times 10^4$ CFU/mL.

MIC_0 results (Figure 4.3) against *S. aureus* for all four series showed that activity generally improved (MIC_0 decreased) with chain length. The longer homologues of **3CCbn** and **3CUrn** (**n** = 20, 22) have reached a plateau in activity. The most active amphiphile against *S. aureus* was **2CAm21** with an MIC_0 of 2.0 ± 1.0 μM. For comparison, vancomycin has an MIC_0 of 0.17 μM.

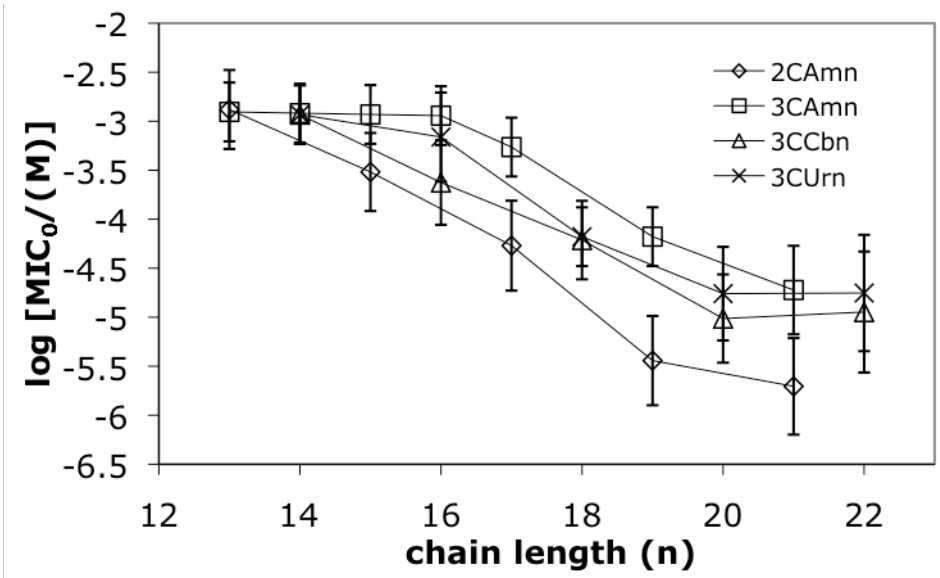

Figure 4.3 MIC_0 comparison for *S. aureus*. Error bars (±0.3) represent one two-fold dilution where multiple determinations of the MIC gave the same value. In cases where different values were obtained the average is reported and ± (log standard of the mean) is added to ±0.3. Lines connecting symbols are eye guides.

MIC_0 results (Figure 4.4) against MRSA for all four series showed that activity generally increased with chain length. The longer homologues of **3CCbn, 3CUrn** (**n** = 20, 22) and **2CAmn** (**n** = 19, 21) amphiphiles have reached a plateau in activity. The

most active amphiphile against *S. aureus* is **3CCb20** with an MIC_0 of 2.9 ± 1.0 μM. For comparison, vancomycin has an MIC_0 of 0.17 μM.

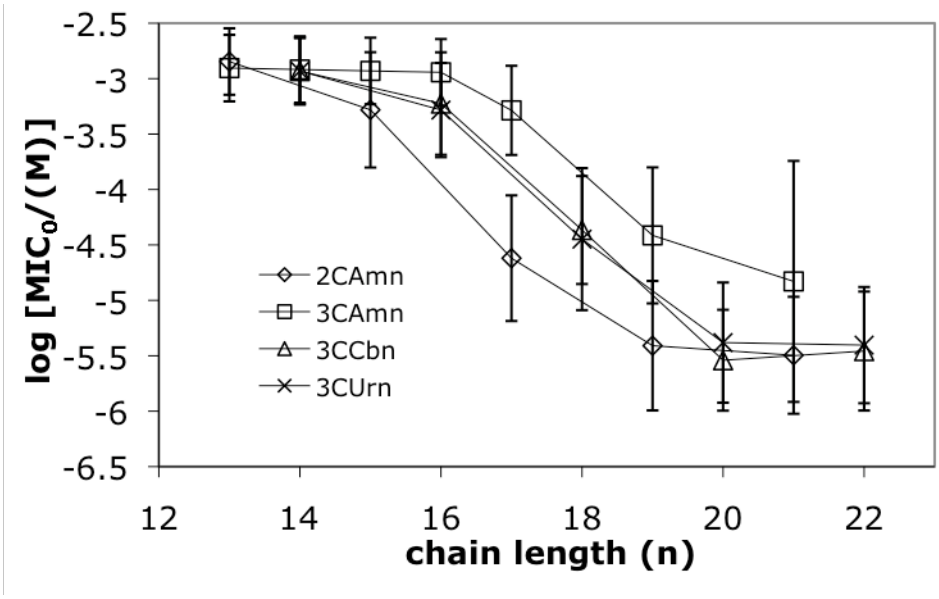

Figure 4.4 MIC_0 comparison for MRSA. Error bars (±0.3) represent one two-fold dilution where multiple determinations of the MIC gave the same value. In cases where different values were obtained the average is reported and ± (log standard of the mean) is added to ±0.3. Lines connecting symbol are eye guides.

4.3 Discussion

4.3.1 MIC_0 Comparison

Comparing the MIC_0s for the **2CAmn** series to those for the three-headed amphiphiles (**3CAmn**, **3CUrn**, **3CCbn**) shows that **2CAm21** is the most active (MIC_0 2.1 ± 1.0 μM) against *S. aureus* (Figure 4.3). It seems that biological activity depends on the number of carboxyl groups comprising the headgroup of the amphiphile. It is important to note that for the **2CAmn** and **3CAmn** series, the MIC_0s are still decreasing with longer chain length (no plateau has been reached). This trend suggests that longer chain (> C_{21}) homologues of **2CAmn** and **3CAmn** may be more active.

Comparing the MIC_0s of all amphiphile series (**2CAmn**, **3CAmn**, **3CUrn**, **3CCbn**) against MRSA (Figure 4.4) shows that the most active amphiphile is **3CCb20** (MIC_0 3.0 ± 1.0 μM). Comparing the **2CAmn** and **3CAmn** series, we can see that the two-headed amphiphiles are more active. As with the *S. aureus* experiments, we can see that the MIC_0s for the **3CAmn** series are still decreasing against MRSA. This trend suggests that longer (> C_{21}) homologues of **3CAmn** amphiphiles may be more active.

4.3.2 Hydrophobicity and Activity

To better understand the activity of our amphiphiles, it is important to understand how hydrophobicity may influence activity. As discussed in the Introduction, the hydrophobicity of the amphiphiles can be compared by using clogp, the logarithm of the calculated partition coefficient. This value describes how a compound partitions between two immiscible solvents (octan-1-ol and water). A web-based program was used to calculate clogp for each of the desired microspecies[6].

The question arises as to which clogp to use, as dendritic amphiphiles exist as several microspecies. Figure 4.5 shows the ionization equilibria (K_a's) in water at pH 7.4 (physiological pH) for **3CAm21** and **2CAm21**; the calculated K_a's in water are shown above the equilibrium arrows[6]. The clogp's are given in parentheses for each ionization state (microspecies)[6]. The most hydrophilic microspecies for **3CAm21** is the trianion (clogp, –3.9) and for **2CAm21** is the dianion (clogp, 0.1). The dianion for **3CAm21** (clogp, –0.3) has a similar value to that of the dianion for **2CAm21**. Likewise the monoanion of **3CAm21** and **2CAm21** have similar clogp's as do the neutral microspecies. The monoanion and neutral species of both **3CAm21** and **2CAm21** are hydrophobic (clogp, >3.0) and would be expected to partition into cell membranes. The

calculations predict that the dominant microspecies (>99%) at pH 7.4 for **3CAm21** and **2CAm21** are the trianion and dianion, respectively.

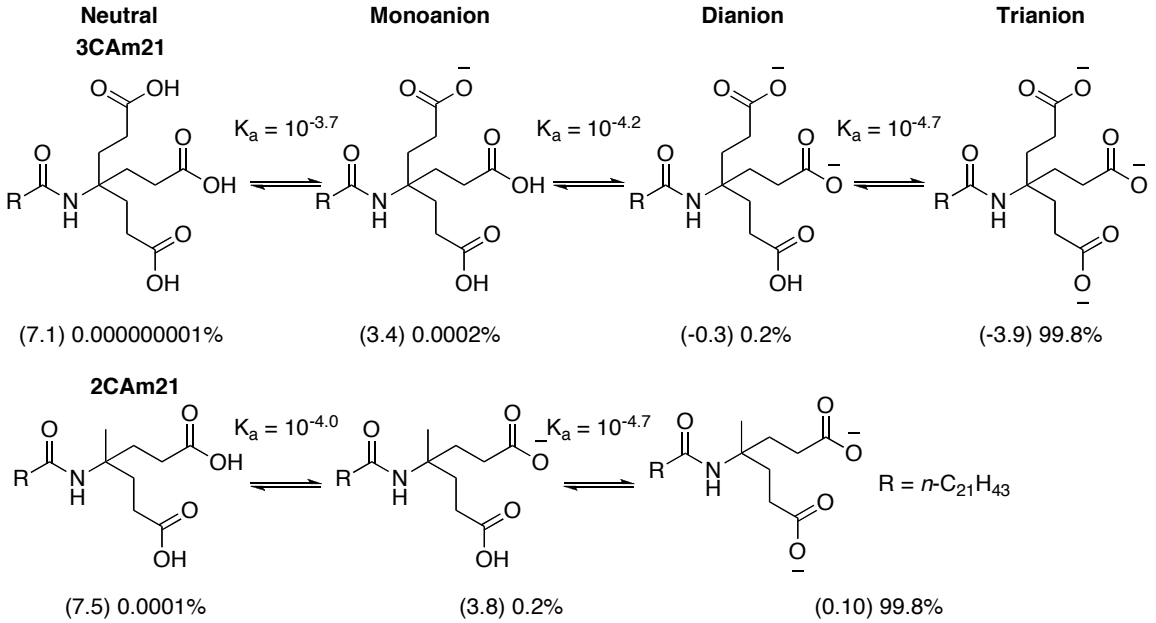

Figure 4.5 Ionization equilibrium for **3CAm21** and **2CAm21**

Equilibrium exists among all the microspecies (Figure 4.5); any microspecies that partitions into a cell (and does not return to aqueous solution) would be re-generated in aqueous solution to re-establish the equilibrium (Le Châtelier's Principle). For example, the most hydrophobic microspecies (the neutral), which is available in trace amounts in aqueous solution at pH 7.4, can partition into a cell and be regenerated in solution.

Plots of MIC_0 versus clogp of the monoanionic microspecies show good agreement among the four series for both *S. aureus* (Figure 4.6) and MRSA (Figure 4.7). In both figures, a plot of MIC_0 versus clogp for the **2CAmn** series is superimposed on those for the **3CAmn**, **3CCbn**, and **3CUrn** series. Although we chose to plot MIC_0 versus clogp of the monoanionic microspecies, plots of MIC_0 versus clogp (not shown) of the neutrals or the dianions give identical patterns to those in Figures 4.6 and 4.7.

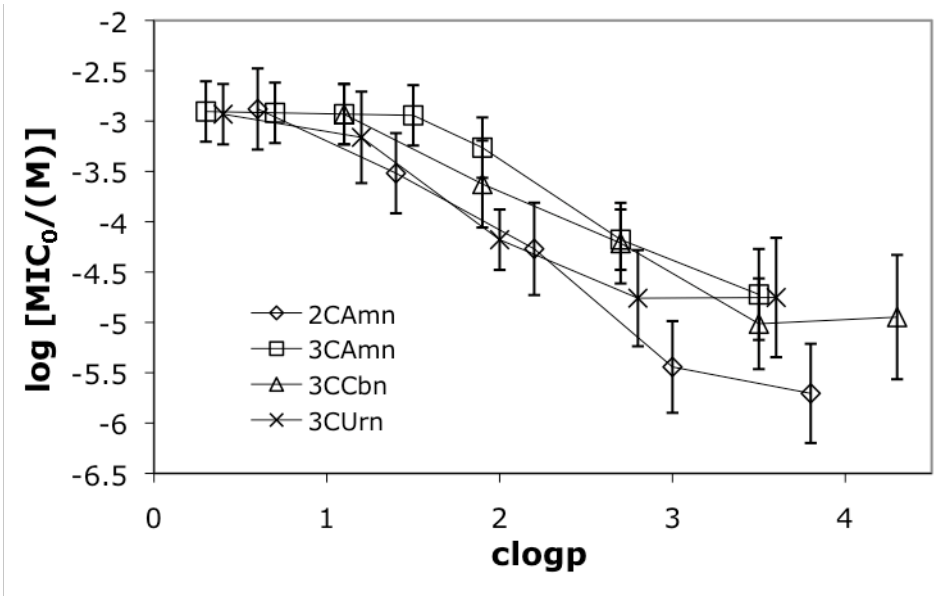

Figure 4.6 MIC_0 against *S. aureus* versus clogp for monoanions of the various amphiphiles. Lines connecting symbols are eye guides.

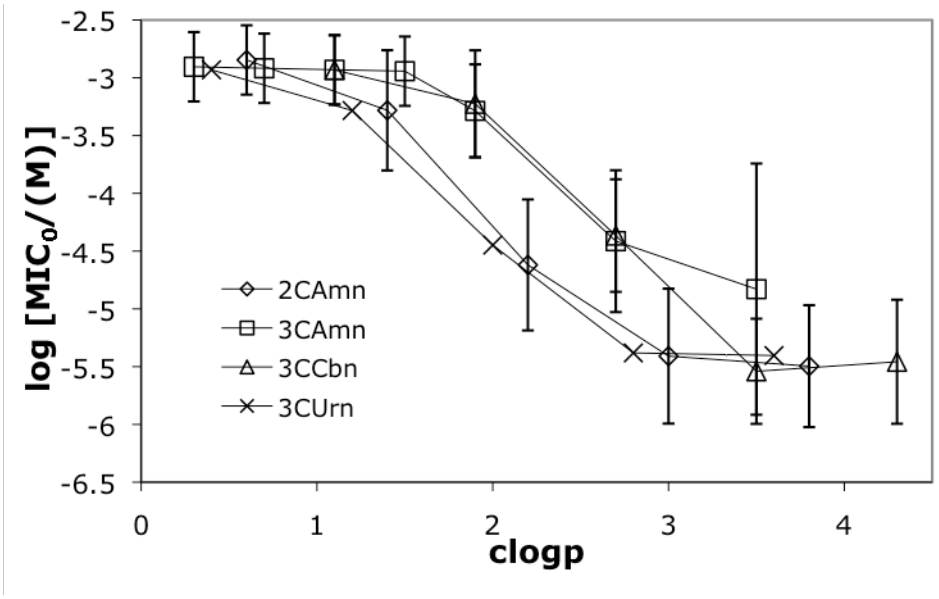

Figure 4.7 MIC_0 against MRSA versus clogp for monoanions of the various amphiphiles. Lines connecting symbols are eye guides.

Comparing Figures 4.3 and 4.4 and Figures 4.6 and 4.7, respectively, suggests that clogp is a better predictor of activity than chain length because the data are clustered more tightly in the latter figures. Log MIC_0 against MRSA has a curvilinear association with clogp (Figure 4.7) regardless of the number of carboxyls and the type of linker–**Am**,

Cb, **Ur**. Log MIC_0 against *S. aureus* also has a similar association (Figure 4.6); however, **2CAm19** and **2CAm21** are more active than the others.

LogD (logarithm of the distribution coefficient) is another parameter often used to estimate the distribution of a compound in an octan-1-ol/water model. LogD is a weighted average of clogp's of all microspecies at a given pH. In our case we are interested in logD's at pH 7.4.

Figure 4.8 shows the difference in logD values for the two- and three-headed amphiphiles for activity against *S. aureus*. From this figure we can see a large gap between the two- and three-headed amphiphiles. A plot (not shown) of logD versus log [MIC/(M)] against MRSA gives a similar pattern. LogD is not used to compare the two- and three-headed amphiphiles because logD can only be predictive for a given structural template. Subtracting a carboxyl group from the dendritic headgroup resets the starting point for logD, thus, making it unlikely to be predictive for these dendritic amphiphiles. If logD were a predictive parameter of activity, one would expect that the most hydrophilic **2CAmn** amphiphile (**2CAm13**) would have similar activity to the most hydrophobic homologues of the three-headed amphiphiles.

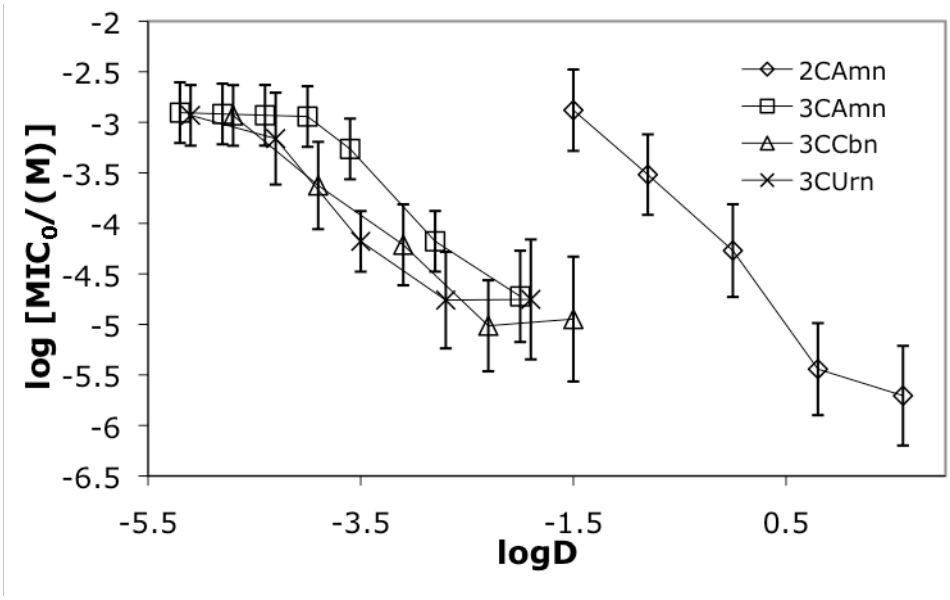

Figure 4.8 MIC_0 versus logD at pH 7.4 for two- and three-headed amphiphiles against *S. aureus*. Lines connecting symbols are eye guides.

4.3.3 Comparison Between CMC and MIC_0

As discussed in Chapter 1 and Chapter 3, we desire to make amphiphiles with high antimicrobial activity (low log MIC_0) and high CMCs (higher log CMC). The CMC value can be used as a measure of the toxicity of an amphiphile[7]. Having a high CMC means that detergency will only be observed at high concentrations. Plotting CMCs versus MIC_0s against *S. aureus* and MRSA for **2CAmn** and **3CAmn** (Figure 4.9) reveals that there is significant difference between CMC and MIC_0. Table 4.1 shows the concentration difference between CMC and MIC_0. These data suggest that detergency is not a likely mechanism of action for antibacterial activity.

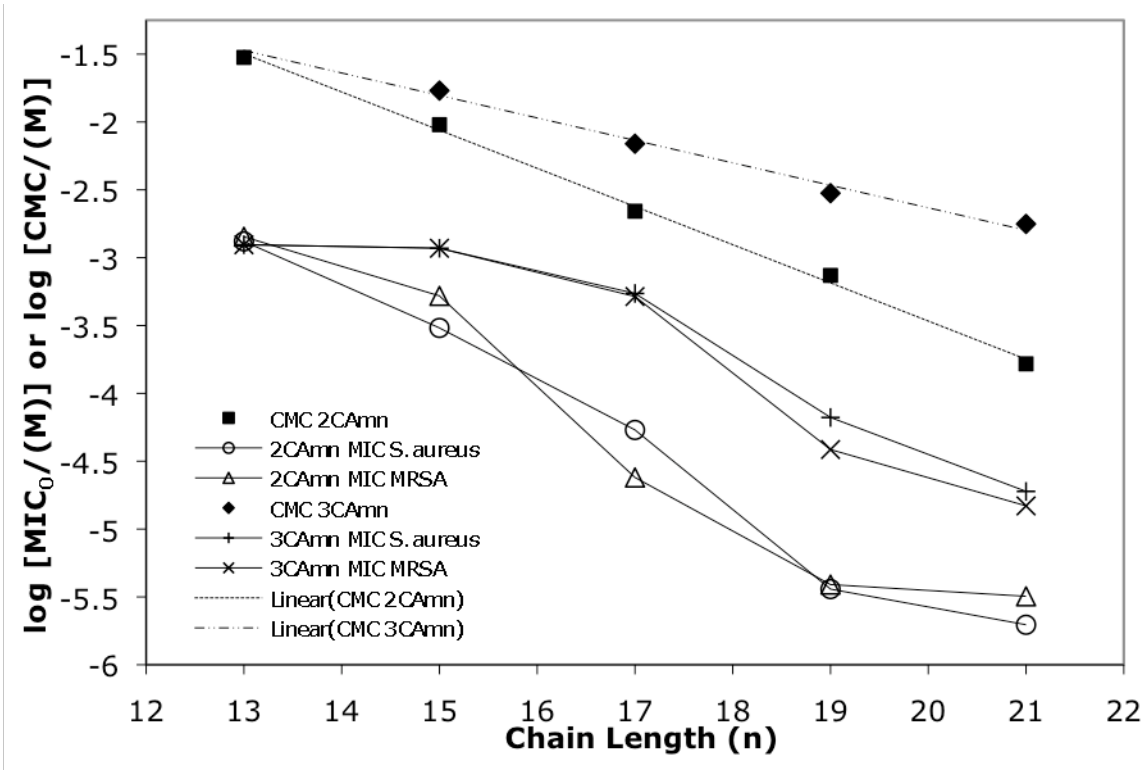

Figure 4.9 CMC and MIC_0 comparison for **2CAmn** and **3CAmn**. Lines connecting MIC_0 symbols are eye guides.

Table 4.1 Concentration ratio (CMC/MIC_0) between CMC and MIC_0

Amphiphile	*S. aureus*	MRSA
3CCb20	54	183
3CCb22	22	72
3CUr20	81	339
3CUr22	57	256
3CAm19	45	76
3CAm21	94	120
2CAm19	205	190
2CAm21	84	52

From the observations above, **2CAm19** may be the best amphiphile against *S. aureus*. Amphiphile **2CAm19** has a high MIC_0, similar to **2CAm21**, and has the largest difference between CMC and MIC_0. This characteristic suggests that **2CAm19** may be the least toxic towards human cells while retaining a similar activity to **2CAm21**. A similar argument can be made for **3CUr20** against MRSA. Amphiphile **3CUr20** has

good activity (MIC_0 4.2 μM) and the largest difference between CMC and MIC_0, which suggests that **3CUr20** may be the best compound against MRSA with a good balance of activity and CMC.

With the MIC_0 values levelling off for **2CAmn**, one could see that with longer chain lengths, the difference between CMC and MIC_0 will decrease. This suggests that detergency may play a roll in the antimicrobial activity of longer amphiphiles.

4.4 Conclusion

Amphiphiles **2CAm19** and **2CAm21** completely inhibit the growth of both *S. aureus* and MRSA. Along with the antibacterial activity of the **2CAmn** series, the CMCs are higher than the MIC_0, which reduces the likelihood that detergency is part of the mechanism of action. From the inoculum density study above (Figures 4.1 and 4.2, respectevily), **2CAm21** becomes less effective (higher log MIC_0) as the cell density of *S. aureus* and MRSA increases. This inoculum effect suggests that these amphiphiles may be less effective against bacteria in high densities, such as in abscesses. The amphiphiles may be more effective in a prophylactic role to help prevent infections.

The two- and three-headed amphiphiles warrant further study towards development as antibiotics, for example as topically applied microbicides that would prevent colonization and transmission of *S. aureus* or MRSA. Other structural templates could be tested for biological activity by modifying the tail and headgroup of the amphiphile. Incorporating double bonds into the tail may increase the biological activity[8] and having a branched chain may increase the CMC to reduce any detergent effect.

4.5 References for Chapter 4

1. Borick, P.M., Bratt, M., Wilson, A. G., Weintraub, L., Kuna, M., *Microbiological activity of certain saturated and unsaturated fatty acid salts of tetradecylamine and related compounds.* Appl. Microbiol, 1959. **7**: p. 248-251.
2. Kabara, J.J., Swieczkowski, D. M., Conley, A. J., Truant, J. P., *Fatty acids and derivatives as antimicrobial agents.* Antimicrob. Agents Chemother., 1972. **2**: p. 23-28.
3. Kabara, J.J., Vrable, R., Lie Ken Jie, M. S. F., *Antimicrobial lipids: natural and synthetic fatty acids and monoglycerides.* Lipids, 1977. **12**: p. 753-759.
4. Li, R.C., Ma, H. H. M., *Parameterization of inoculum effect via mathematical modeling: aminoglycosides against Staphylococcus aureus and Escherichia coli.* J. Chemother, 1998. **10**: p. 203-207.
5. Sugandhi, E.K., Macri, R. V., Williams, A. A., Kite, B. L., Slebodnick, C., Falkinham, J. O. III, Esker, A. R., Gandour, R. D., *Synthesis, critical micelle concentration, and antimycobacterial properties of homologous dendritic amphiphiles. Probing intrinsic activity and the "cutoff" effect.* J. Med. Chem., 2007. **50**: p. 1645-1650.
6. *Marvin Sketch 5.0.0. pKa, logP, and logD calculator*. ChemAxon [cited February 1, 2008]; Available from: http://intro.bio.umb.edu/111-112/OLLM/111F98/newclogp.html.
7. Vieria, O.V., Hartmann, D. O., Cardoso, C. M. P., Oberdoerfer, D., Baptista, M., Santos, M. A. S., Almeida, L., Ramalho-Santos, J., Vaz, W. L. C., *Surfactants as microbicides and contraceptive agents: a systematic in vitro study*. PLoS One, 2008. **3**(8): p. e2913.
8. Ohta, S., Shiomi, Y., Kawashima, A., Aozasa, O., Nakao, T., Nagate, T., Kitamura, K., Miyata, H., *Antibiotic effect of linolenic acid from chlorococcum strains Hs-101 and dunaliella-primolecta on methicillin-resistant staphylococcus aureus.* J. Appl. Phycol., 1995. **7**(2): p. 121-127.

Chapter 5: Summary and Conclusion

5.1 Summary

The syntheses of nitrodiester, diesteramine, **2EAm13**, **2EAm15**, **2EAm17**, **2EAm19**, **2EAm21**, **2CAm13**, **2CAm15**, **2CAm17**, **2CAm19**, and **2CAm21** have been successful. A new method was used for the preparation of the nitrodiester synthon; the diesteramine was prepared by a published method[1]. All five **2EAmn** and five **2CAmn** amphiphiles have been fully characterized by ^{1}H NMR, ^{13}C NMR, IR, high-resolution mass spectroscopy, and elemental analysis.

The CMC values for the five **2CAmn** amphiphiles were measured to establish the concentration required for detergency. The **2CAmn** CMCs were found to decrease in value from 3.0×10^{-2} M (**2CAm13**) to 1.7×10^{-4} M (**2CAm21**) in a linear fashion [log CMC = $(-0.28 \pm 0.01)\mathbf{n} + (2.2 \pm 0.1)$]. The CMCs values for the **2CAmn** series are lower than the three series of three-headed amphiphiles (**3CAmn**, **3CCbn**, **3CUrn**) and higher than fatty acids.

The MIC results revealed that inoculum density, chain-length, and hydrophobicity all influenced antibacterial activity and that activity correlates strongly with clogp. The most hydrophobic members from each homologous series exhibited antibacterial activity. The most active amphiphile against *S. aureus* was **2CAm21** (MIC_0 2.0 ± 1.0 μM) and the most active against MRSA was **3CCb20** (MIC_0 2.9 ± 1.0 μM). For comparison, vancomycin has an MIC_0 of 0.17 μM.

The CMCs and MICs of the two- and three-headed amphiphiles were compared for both *S. aureus* and MRSA to gauge the effect that micelles may have on activity. Amphiphile **2CAm19** has the largest ratio between CMC and MIC_0 ($CMC/MIC_0 = 205$)

against *S. aureus* and **3CUr20** has the largest ratio ($CMC/MIC_0 = 339$) against MRSA. Even though **2CAm19** and **3CUr20** are not the most active amphiphiles, they may be the best candidates for further development because of the larger gaps between CMC and MIC_0. These large gaps may suggest that the two amphiphiles are less cytotoxic. These high ratios suggest that micelle formation is not a likely mechanism of action for activity.

5.2 Conclusion

The longer homologues of the **2CAmn** series completely inhibit the growth of both *S. aureus* and MRSA. Along with the antibacterial activity of the **2CAmn** series, the CMCs are higher than the MIC_0, which reduces the likelihood that cytotoxicity or irritation is caused by micelle formation. From the inoculum density study (Chapter 4), **2CAm21** becomes less effective (higher log MIC_0) as the cell density of *S. aureus* and MRSA increases. This inoculum effect suggests that these amphiphiles may be less effective against bacteria in high densities, such as in abscesses. The amphiphiles may be more effective in a prophylactic role to help prevent infections.

The two- and three-headed amphiphiles warrant further study towards development as antibiotics, for example as topically applied microbicides that would prevent colonization and transmission of *S. aureus* or MRSA. Other structural templates could be tested for biological activity by modifying the tail and headgroup of the amphiphile. Although longer homologues may be more active, the CMCs will be lower as well. This would lead to lower CMC/MIC_0 ratios. Incorporating double bonds or branching into the fatty tail should increase the CMC and might lower the MIC_0. As such, these compounds would have higher CMC/MIC_0 ratios and consequently lower potential cytotoxicity due to detergency.

5.3 References for Chapter 5

1. Newkome, G.R., He, E., Godinez, L. A., Baker, G. R., *Electroactive metallomacromolecules via tetrabis(2,2':6',2"-terpyridine)ruthenium(II) complex: dendritic nanonetworks towards constitutional isomers and neutral species without external counterions.* J. Am. Chem. Soc., 2000. **122**: p. 9993-10006.